ChemSusChem

Supporting Information

Polar Substitutions on the Surface of a Lipase Substantially Improve Tolerance in Organic Solvents

Haiyang Cui, Markus Vedder, Lingling Zhang, Karl-Erich Jaeger, Ulrich Schwaneberg,* and Mehdi D. Davari*

Supporting Information

Polar substitutions on the surface of a lipase substantially improve tolerance in organic solvents

Haiyang Cui[1,2†], Markus Vedder[1], Lingling Zhang[3], Can Bora Yildiz[1], Karl-Erich Jaeger[4,5], Ulrich Schwaneberg[1,2], Mehdi D. Davar[6,*]*

[1]Institute of Biotechnology, RWTH Aachen University, Worringerweg 3, Aachen 52074, Germany

[2]DWI-Leibniz Institute for Interactive Materials, Forckenbeckstraße 50, Aachen 52074, Germany

[3]Tianjin Institute of Industrial Biotechnology, Chinese Academy of Sciences, West 7th Avenue 32, Tianjin Airport Economic Area, Tianjin 300308, China

[4]Institute of Molecular Enzyme Technology, Heinrich Heine University Düsseldorf, Wilhelm Johnen Strasse, Jülich 52426, Germany

[5]Institute of Bio-and Geosciences IBG 1: Biotechnology, Forschungszentrum Jülich GmbH, Wilhelm Johnen Strasse, Jülich 52426, Germany

[6]Department of Bioorganic Chemistry, Leibniz Institute of Plant Biochemistry, Weinberg 3, 06120 Halle, Germany

[†]Current address: University of Illinois at Urbana-Champaign, Carl R. Woese Institute for Genomic Biology, 1206 West Gregory Drive, Urbana, IL 61801

*Corresponding Author: Dr. Mehdi D. Davari

Prof. Dr. Ulrich Schwaneberg

Table of Contents

Overall structure dynamics and solvation behaviors in BSLA substitutions 6

Energy interaction behaviors on the substituted site 7

Conformational and solvation change in the substrate binding cleft 8

Table S1. Summary of calculated observables during MD simulation 9

Table S2. Property of the selected fifteen non-beneficial substitutions 11

Table S3. Property of the selected thirty beneficial substitutions 12

Table S4. The averaged non-bond binding energy between the overall structure of BSLA variants and DMSO molecules 14

Table S5. The averaged non-bond binding energy between the overall structure of BSLA variants and Water molecules 15

Table S6. The averaged non-bond binding energy between the substituted site and DMSO molecules 16

Table S7. The averaged non-bond binding energy between the substituted site and water molecules 17

Table S8. Analysis of 1267 polar substitution that all type of amino acid substitute to polar residue towards OSs resistance in BSLA-SSM library 18

Table S9. Analysis of the 364 non-polar substitutions that polar amino acid substitute to non-polar residue towards OSs resistance in BSLA-SSM library. 19

Table S10. Analysis of the 896 surface polar substitutions that all type of amino acid substitute to polar residue towards OSs resistance in BSLA-SSM library. 20

Table S11. Analysis of the surface polar substitutions that different amino acid substitute to polar residue towards OSs resistance in BSLA-SSM library. 21

Figure S1. Root-mean-square deviation (RMSD) of the BSLA non-beneficial substitutions backbone with respect to the initial structure as a function of time in 60 % (v/v) DMSO 22

Figure S2. Root-mean-square deviation (RMSD) of the BSLA beneficial substitutions (group 1) backbone with respect to the initial structure as a function of time in 60 % (v/v) DMSO 23

Figure S3. Root-mean-square deviation (RMSD) of the BSLA beneficial substitutions (group 2) backbone with respect to the initial structure as a function of time in 60 % (v/v) DMSO 24

Figure S4. Time-average RMSD of BSLA non-beneficial and beneficial substitutions determined from the last 40 ns of simulations in 60 % (v/v) DMSO. 25

Figure S5. Thermodynamic stability ($\Delta\Delta G_{fold}$) of BSLA beneficial and non-beneficial substitutions 26

Figure S6. The time-averaged radius of gyration (R_g) of BSLA non-beneficial and beneficial substitutions in 60 % (v/v) DMSO..... 27

Figure S7. The number of internal hydrogen bonds with > 95% occupancy in BSLA beneficial and non-beneficial substitutions in 60 % (v/v) DMSO..... 28

Figure S8. The time-averaged (**a**) total (**b**) hydrophobic (**c**) hydrophilic SASA of BSLA beneficial and non-beneficial substitutions in 60 % (v/v) DMSO 29

Figure S9. Hydration shell of BSLA beneficial and non-beneficial substitutions in 60 % (v/v) DMSO during MD simulations..... 30

Figure S10. DMSO solvation layer of BSLA the non-beneficial and beneficial substitution in 60 % (v/v) DMSO during MD simulations..... 31

Figure S11. The average number of water molecules around the BSLA substituted residue during the MD simulations in 60 % (v/v) DMSO 32

Figure S12. Contacts frequency of substituted sites between the BSLA beneficial substitution (group 2) and (**a**) water, (**b**) DMSO molecule in 60 % (v/v) DMSO, respectively 33

Figure S13. Contacts frequency between each BSLA residue and DMSO towards non-beneficial and beneficial substitutions in 60 % (v/v) DMSO 34

Figure S14. Contacts frequency between each BSLA residue and water towards non-beneficial and beneficial substitutions in 60 % (v/v) DMSO 35

Figure S15. RMSF of each residue of BSLA non-beneficial substitutions determined from the last 40 ns of MD simulations in 60 % (v/v) DMSO 36

Figure S16. RMSF of each residue of BSLA beneficial substitutions (group 1) determined from the last 40 ns of MD simulations in 60 % (v/v) DMSO..... 37

Figure S17. RMSF of each residue of BSLA beneficial substitutions (group 2) determined from the last 40 ns of MD simulations in 60 % (v/v) DMSO..... 38

Figure S18. The RMSF of the substituted residue of BSLA beneficial substitutions (group 2) in 60 % (v/v) DMSO 39

Figure S19. The SASA of the substituted residue of BSLA beneficial and non-beneficial substitutions in 60 % (v/v) DMSO during MD simulations 40

Figure S20. Averaged distance between substituted residue and the catalytic triad (**a**) Ser77, (**b**) Asp133, (**c**) His156 of BSLA beneficial and non-beneficial substitutions in 60 % (v/v) DMSO 41

Figure S21. Conformational and solvation change in the substrate binding cleft 42

Figure S22. The averaged internal-atomic distance between the catalytic triad (Ser77, His156, Asp133) and oxyanion hole (Ile12, Met78) of BSLA beneficial and non-beneficial substitutions 43

Figure S23. The average number of solvent molecules in substrate binding cleft of BSLA beneficial and non-beneficial substitutions during the MD simulations 44

Figure S24. DOX resistance heatmap of BSLA surface polar-related substitutions 45

Figure S25. TFE resistance heatmap of BSLA surface polar-related substitutions..... 46

Overall structure dynamics and solvation behaviors in BSLA substitutions

As shown in Figure S1-S4, the structures of both beneficial and non-beneficial BSLA variants were maintained in DMSO throughout the time evolution. 36.7 % (11/30) beneficial polar substitutions displayed reduced RMSD value (**Figure 1b** and **S4**), indicating that the whole BSLA structure becomes more stable in DMSO comparing to non-beneficial ones. However, there are 40.0 % (12/30) and 23.3 % (7/30) of beneficial variants showing comparable and increased RMSD value, respectively. Similar results were confirmed by thermodynamic stability analysis (**Figure 1b** and **Figure S5**). The R_g was nearly 12.5 Å for all BSLA variants and only had little difference in first decimal place. The fluctuations of R_g in 47 % (14/30) variants were in the same range (beneficial = non-beneficial, **Figure 1b** and **S6**). The latter indicates little variation structural compactness within BSLA variants in DMSO. Similar observation was shown in terms of internal H-bond that 56.7 % (17/30) was equal for beneficial and non-beneficial substitutions (**Figure 1b**, and **S7**). 76.7 % had unchanged even decreased total SASA compared to non-beneficial, which mainly coming from the lower hydrophobic SASA (46.7 %) but similar hydrophilic SASA (46.7 %) in **Figure 1b** and **S8**.

Energy interaction behaviors on the substituted site.

Furthermore, energy-based factors, including the non-bond binding free energies ($\Delta G_{\text{non-bond}}$), electrostatic energy (ΔE_{elec}), and van der Waals force (ΔE_{vdW}), were calculated to examine the strength of water/OS molecule binds to BSLA substituted site (**Figure 3a** and **Table S6-S7**). 63 % (19/30) and 70 % (21/30) variants present inferior $\Delta G_{\text{non-bond}}$ value of non-bond DMSO and superior ΔE_{elec} value of residue-water, respectively, which indeed correlating to the above solvation founding. The result of interaction energies demonstrated that DMSO molecules in beneficial polar substitutions interact the enzyme more slightly than non-beneficial ones. Oppositely, water binds more tightly.

Conformational and solvation change in the substrate binding cleft

The distance between substitution positions and catalytic triad (S77, D133, H156) were varied from 6.3 Å to 32.7 Å (**Figure S20**). The overview of conformational and solvation change in the substrate binding cleft was shown in **Figure S21**. In detail, the Asp133-OD1⋯His156-ND1 distance did not show a obvious change in 84 % BSLA beneficial substitutions (**Figure S21** and **S22**), suggesting that the original H-bond (around 3.5 Å) between Asp133 and His156 is very stable in BSLA.[1] As previous founding,[2] the catalytically relevant H-bond between Ser77-OG and His156-NE2 of BSLA in DMSO was mostly broken because the distance increased from ~4.5 Å in water to 4.6-12.0 Å (**Figure S21** and **S22**).[1] 43 % beneficial substitutions had an increased Ser77-OG⋯His156-NE2 distance. But 50 % Ile12-N⋯Met78-N (oxyanion hole) showed decreased distance value, which would disturb the stabilization state of negatively charged reaction intermediates and/or the substrate specificity.[1] Almost comparable solvation phenomenon are happened in the substrate binding cleft with ranging 54-77 %(**Figure S21** and **S23**).

Table S1. Summary of calculated observables during MD simulation.

Descriptor	Location	Observables	Results
Overall protein	Geometrical property	Time-averaged RMSD	Fig. 1b, S1-S4
		Time-averaged R_g	Fig. 1b, S6
		Internal H-bond	Fig. 1b, S7
		Thermodynamic stability	Fig. 1b, S5
		Total SASA	Fig. 1b, S8a
		Hydrophobic SASA	Fig. 1b, S8b
		Hydrophilic SASA	Fig. 1b, S8c
	Solvation phenomenon	DMSO layer	Fig. 1b, S10
		Hydration shell	Fig. 1b, S9
		BSLA-DMSO contact frequency	Fig. 1b, 1c
		BSLA-Water contact frequency	Fig. 1b, 1d
	Interaction energy	ΔE_{vdW} (BSLA-DMSO)	Fig. 1b, Tab. S4
		ΔE_{elec} (BSLA-DMSO)	Fig. 1b, Tab. S4
		$\Delta G_{non\text{-}bond}$ (BSLA-DMSO)	Fig. 1b, Tab. S4
		ΔE_{vdW} (BSLA-Water)	Fig. 1b, Tab. S5
		ΔE_{elec} (BSLA-Water)	Fig. 1b, Tab. S5
		$\Delta G_{non\text{-}bond}$ (BSLA-Water)	Fig. 1b, Tab. S5
Substitution site	Geometrical property	SASA of residue	Fig. 3a, S19
		RMSF of residue	Fig. 3b, S15-S18,
		Distance of substitution⋯Ser77	Fig. 3a, S20a
		Distance of substitution⋯Asp133	Fig. 3a, S20b
		Distance of substitution⋯His156	Fig. 3a, S20c
	Solvation phenomenon	Number of DMSO molecule	Fig. 3a, 3b
		Number of Water molecule	Fig. 3a, S11
		Residue-DMSO contact frequency	Fig. 4, S12, S13
		Residue-Water contact frequency	Fig. 4, S12, S14
	Interaction energy	ΔE_{vdW} (Residue-DMSO)	Fig. 3a, Tab. S6
		ΔE_{elec} (Residue-DMSO)	Fig. 3a, Tab. S6
		$\Delta G_{non\text{-}bond}$ (Residue-DMSO)	Fig. 3a, Tab. S6
		ΔE_{vdW} (Residue-Water)	Fig. 3a, Tab. S7

Descriptor	Location	Observables	Results
		ΔE_{elec} (Residue-Water)	Fig. 3a, Tab. S7
		$\Delta G_{non\text{-}bond}$ (Residue-Water)	Fig. 3a, Tab. S7
Active site	Geometrical property	Distance of His156-ND1⋯Asp133-OD1	Fig. S21, S22c
		Distance of Ser77-OG⋯His156-OD2	Fig. S21, S22b
		Distance of Ile12-N⋯Met78-N	Fig. S21, S22a
	Solvation phenomenon	Number of DMSO molecule	Fig. S21, S23a
		Number of Water molecule	Fig. S21, S23b
		SBC-DMSO contact frequency[a]	Fig. S13
		SBC-Water contact frequency[a]	Fig. S13
In total		39	

[a]Substrate binding cleft is donated as SBC.

Table S2. Property of the selected fifteen non-beneficial substitutions

Surface Substitution[a]		Secondary structure[b]	Specific activity relative to WT[c]	Resistance relative to WT
Non-beneficial	N4I	loop	1.13 ± 0.12	0.7 ± 0.07
	I12G	turn	0.06 ± 0.01	0.0
	G14F	loop	1.18 ± 0.12	0.3 ± 0.03
	A15W	loop	1.20 ± 0.13	0.6 ± 0.06
	F17W	3/10-helix	1.55 ± 0.16	1.0 ± 0.10
	G93Y	3/10-helix	1.37 ± 0.14	1.0 ± 0.10
	N94W	3/10-helix	0.80 ± 0.08	0.8 ± 0.08
	K95I	loop	1.01 ± 0.11	1.1 ± 0.12
	M137F	loop	0.89 ± 0.09	0.9 ± 0.09
	L140Y	α-helix	1.76 ± 0.18	0.9 ± 0.09
	G145V	loop	0.22 ± 0.02	0.9 ± 0.09
	Q150W	Beta strand	1.45 ± 0.15	0.9 ± 0.09
	L168I	α-helix	0.22 ± 0.02	0.7 ± 0.07
	G175W	turn	0.90 ± 0.09	0.9 ± 0.09
	G177I	loop	0.87 ± 0.09	0.9 ± 0.09

[a] Relative location assignment to the sequence based on the structure of BSLA WT (PDB ID: 1i6w[3], chain A) was taken from previous work.[4]

[b] Secondary structure data provided by DSSP.[5]

[c] The specific activity of the purified BSLA WT in the absence/presence of 60 % (v/v) DMSO was 11.5 ± 1.2 U/mg and 4.6 ± 0.9 U/mg, respectively. One unit (U) of enzyme activity was defined as the amount of enzyme releasing 1.0 mmol of *p*-nitrophenol per minute under the assay conditions.[6]

Table S3. Property of the selected thirty beneficial substitutions

Surface Substitution[a]		Secondary structure[b]	Specific activity relative to WT[c]	Resistance relative to WT
Beneficial substitutions group 1	N4S	loop	2.11 ± 0.22	1.8 ± 0.19
	I12S	turn	0.22 ± 0.02	2.6 ± 0.27
	G14N	loop	0.24 ± 0.03	1.5 ± 0.16
	A15T	loop	0.65 ± 0.07	1.4 ± 0.15
	F17M	3/10-helix	1.23 ± 0.13	1.6 ± 0.17
	G93M	3/10-helix	0.83 ± 0.09	1.3 ± 0.14
	N94M	3/10-helix	1.27 ± 0.13	1.3 ± 0.14
	K95S	loop	1.62 ± 0.17	1.7 ± 0.18
	M137P	loop	1.87 ± 0.19	1.5 ± 0.16
	L140S	α-helix	0.74 ± 0.08	1.6 ± 0.17
	G145M	loop	0.68 ± 0.07	1.5 ± 0.16
	Q150T	Beta strand	1.43 ± 0.15	1.4 ± 0.15
	L168T	α-helix	1.30 ± 0.14	1.4 ± 0.15
	G175S	turn	0.93 ± 0.09	1.4 ± 0.15
	G177T	loop	0.60 ± 0.06	1.4 ± 0.15
Beneficial substitutions group 2	N4T	loop	1.88 ± 0.19	1.7 ± 0.18
	I12T	turn	0.22 ± 0.02	2.3 ± 0.24
	G14Q	loop	0.15 ± 0.02	1.4 ± 0.15
	A15T	loop	0.65 ± 0.07	1.4 ± 0.15
	F17T	3/10-helix	1.31 ± 0.14	1.4 ± 0.15
	G93P	3/10-helix	2.44 ± 0.26	1.9 ± 0.19
	N94P	3/10-helix	1.34 ± 0.14	1.3 ± 0.14
	K95N	loop	1.59 ± 0.17	1.8 ± 0.19
	M137T	loop	0.86 ± 0.09	1.3 ± 0.14
	L140T	α-helix	0.87 ± 0.09	1.6 ± 0.17
	G145Q	loop	1.47 ± 0.15	2.0 ± 0.21
	Q150N	Beta strand	1.44 ± 0.15	1.6 ± 0.17
	L168N	α-helix	1.44 ± 0.15	1.5 ± 0.16
	G175T	turn	0.98 ± 0.10	1.4 ± 0.15
	G177Q	loop	1.3 ± 0.14	1.5 ± 0.16

[a]. Relative location assignment to the sequence based on the structure of BSLA WT (PDB ID: 1i6w[3], chain A) was taken from previous work.[4]
[b]. Secondary structure data provided by DSSP.[5]

[c] The specific activity of the purified BSLA WT in the absence/presence of 60 % (v/v) DMSO was 11.5 ± 1.2 U/mg and 4.6 ± 0.9 U/mg, respectively. One unit (U) of enzyme activity was defined as the amount of enzyme releasing 1.0 mmol of *p*-nitrophenol per minute under the assay conditions.[6]

Table S4. The averaged non-bond binding energy between the overall structure of BSLA variants and DMSO molecules.[a]

Amino acid Position	Non-beneficial (kcal/mol)			Beneficial group 1 (kcal/mol)			Beneficial group 2 (kcal/mol)		
	ΔE_{vdW}	ΔE_{elec}	$\Delta G_{non\text{-}bond}$	ΔE_{vdW}	ΔE_{elec}	$\Delta G_{non\text{-}bond}$	ΔE_{vdW}	ΔE_{elec}	$\Delta G_{non\text{-}bond}$
4	-2601 ± 131	-2173 ± 140	-4774 ± 270	-2413 ± 70	-1991 ± 29	-4404 ± 84	-2284 ± 119	-1897 ± 80	-4181 ± 169
12	-2470 ± 32	-2009 ± 46	-4479 ± 73	-2294 ± 58	-1871 ± 63	-4166 ± 113	-2371 ± 135	-2056 ± 170	-4427 ± 300
14	-2390 ± 95	-1907 ± 135	-4298 ± 214	-2468 ± 80	-2031 ± 121	-4499 ± 197	-2326 ± 56	-1825 ± 108	-4151 ± 167
15	-2589 ± 63	-2108 ± 92	-4697 ± 180	-2384 ± 93	-1904 ± 148	-4288 ± 231	-2405 ± 50	-1995 ± 23	-4400 ± 36
17	-2475 ± 102	-2000 ± 102	-4474 ± 201	-2274 ± 132	-1899 ± 138	-4173 ± 300	-2245 ± 45	-1806 ± 58	-4051 ± 113
93	-2475 ± 102	-2017 ± 111	-4492 ± 192	-2445 ± 42	-1978 ± 28	-4423 ± 53	-2519 ± 116	-2063 ± 30	-4582 ± 124
94	-2361 ± 119	-1907 ± 117	-4267 ± 202	-2379 ± 97	-1933 ± 110	-4312 ± 194	-2446 ± 139	-2020 ± 165	-4467 ± 286
95	-2502 ± 141	-2058 ± 151	-4560 ± 251	-2301 ± 104	-1840 ± 95	-4141 ± 167	-2402 ± 74	-1963 ± 36	-4365 ± 121
137	-2302 ± 112	-1882 ± 146	-4184 ± 140	-2321 ± 94	-1881 ± 122	-4202 ± 207	-2437 ± 108	-2055 ± 97	-4492 ± 190
140	-2449 ± 180	-2004 ± 173	-4453 ± 342	-2357 ± 141	-1995 ± 204	-4352 ± 352	-2435 ± 111	-2035 ± 72	-4470 ± 194
145	-2319 ± 126	-1842 ± 107	-4160 ± 94	-2444 ± 24	-2025 ± 17	-4469 ± 55	-2323 ± 220	-1903 ± 244	-4226 ± 457
150	-2336 ± 58	-1880 ± 69	-4215 ± 102	-2368 ± 54	-1977 ± 28	-4345 ± 19	-2512 ± 117	-2083 ± 120	-4594 ± 246
168	-2555 ± 36	-2094 ± 11	-4649 ± 120	-2261 ± 81	-1788 ± 29	-4049 ± 96	-2257 ± 54	-1870 ± 60	-4127 ± 99
175	-2383 ± 41	-1930 ± 34	-4313 ± 88	-2402 ± 129	-1952 ± 128	-4355 ± 262	-2622 ± 60	-2203 ± 89	-4825 ± 116
177	-2413 ± 141	-1944 ± 132	-4356 ± 265	-2504 ± 46	-2094 ± 38	-4598 ± 131	-2259 ± 64	-1816 ± 78	-4075 ± 108

[a] The data were averaged from the last 40 ns in three independent MD runs. ΔE_{elec}: electrostatic energy. ΔE_{vdW}: van der Waals. $\Delta G_{non\text{-}bond}$: the non-bond binding. $\Delta G_{non\text{-}bond} = \Delta E_{elec} + \Delta E_{vdW}$.

Table S5. The averaged non-bond binding energy between the overall structure of BSLA variants and Water molecules.[a]

Amino acid Position	Non-beneficial (kcal/mol)			Beneficial group 1 (kcal/mol)			Beneficial group 2 (kcal/mol)		
	ΔE_{vdW}	ΔE_{elec}	$\Delta G_{non\text{-}bond}$	ΔE_{vdW}	ΔE_{elec}	$\Delta G_{non\text{-}bond}$	ΔE_{vdW}	ΔE_{elec}	$\Delta G_{non\text{-}bond}$
4	306 ± 16	-7031 ±279	-6726 ± 272	316 ± 23	-7250 ± 289	-6934 ± 249	308 ± 24	-7139 ± 360	-6832 ± 381
12	320 ± 9	-7220 ± 107	-6901 ± 136	329 ± 14	-7339 ± 150	-7010 ± 145	314 ± 23	-7238 ± 95	-6924 ± 41
14	322 ± 6	-7123 ± 279	-6802 ± 216	333 ± 11	-7297 ± 221	-6964 ± 241	315 ± 19	-7179 ± 93	-6864 ± 62
15	316 ± 21	-7251 ± 204	-6934 ± 198	328 ± 20	-7331 ± 121	-7003 ± 98	317 ± 33	-7178 ± 323	-6861 ± 282
17	339 ± 22	-7208 ± 50	-6869 ± 123	310 ± 11	-7204 ± 138	-6894 ± 136	330 ± 7	-7132 ± 133	-6802 ± 218
93	321 ± 13	-7069 ± 277	-6748 ± 230	334 ± 19	-7335 ± 123	-7001 ± 140	312 ± 15	-7245 ± 62	-6933 ± 88
94	322 ± 27	-7076 ± 122	-6755 ± 79	295 ± 15	-6860 ± 235	-6565 ± 232	304 ± 10	-7123 ± 242	-6819 ± 246
95	307 ± 43	-6952 ± 148	-6645 ± 119	337 ± 2	-7298 ± 62	-6961 ± 84	318 ± 10	-7182 ± 192	-6864 ± 183
137	304 ± 5	-7394 ± 22	-7090 ± 225	284 ± 7	-7022 ± 179	-6738 ± 173	314 ± 23	-7173 ± 272	-6859 ± 322
140	316 ± 19	-7046 ± 98	-6730 ± 105	316 ± 12	-7274 ± 181	-6958 ± 229	318 ± 12	-7234 ± 253	-6916 ± 258
145	304 ± 32	-7033 ± 177	-6729 ± 134	284 ± 41	-6884 ± 168	-6599 ± 146	322 ± 29	-7204 ± 129	-6882 ± 135
150	280 ± 32	-7069 ± 73	-6789 ± 82	335 ± 24	-7141 ± 191	-6805 ± 199	303 ± 15	-7046 ± 269	-6743 ± 220
168	342 ± 23	-7123 ± 246	-6782 ± 115	301 ± 9	-7387 ± 211	-7086 ± 220	309 ± 23	-6990 ± 220	-6682 ± 229
175	326 ± 14	-7154 ± 160	-6828 ± 146	315 ± 13	-6974 ± 51	-6659 ± 48	327 ± 9	-7161 ± 101	-6834 ± 106
177	278 ± 23	-7076 ± 197	-6798 ± 160	341 ± 22	-7361 ± 79	-7020 ± 19	301 ± 18	-7126 ± 145	-6825 ± 146

[a] The data were averaged from the last 40 ns in three independent MD runs. ΔE_{elec}: electrostatic energy. ΔE_{vdW}: van der Waals. $\Delta G_{non\text{-}bond}$: the non-bond binding. $\Delta G_{non\text{-}bond} = \Delta E_{elec} + \Delta E_{vdW}$.

Table S6. The averaged non-bond binding energy between the substituted site and DMSO molecules.[a]

Amino acid Position	Non-beneficial (kcal/mol)			Beneficial group 1 (kcal/mol)			Beneficial group 2 (kcal/mol)		
	ΔE_{vdW}	ΔE_{elec}	$\Delta G_{non\text{-}bond}$	ΔE_{vdW}	ΔE_{elec}	$\Delta G_{non\text{-}bond}$	ΔE_{vdW}	ΔE_{elec}	$\Delta G_{non\text{-}bond}$
4	-14 ± 1	-10 ± 1	-24 ± 1	-7 ± 1	-6 ± 4	-13 ± 1	-10 ± 1	-6 ± 1	-16 ± 1
12	-12 ± 3	-7 ± 4	-18 ± 2	-19 ± 3	-17 ± 12	-36 ± 13	-24 ± 2	-17 ± 7	-42 ± 5
14	-25 ± 12	-7 ± 6	-32 ± 16	-18 ± 5	-24 ± 15	-42 ± 10	-21 ± 10	-24 ± 14	-45 ± 11
15	-51 ± 6	-22 ± 7	-73 ± 10	-19 ± 4	-27 ± 15	-46 ± 10	-14 ± 3	-14 ± 3	-28 ± 5
17	-61 ± 4	-34 ± 7	-95 ± 8	-37 ± 4	-15 ± 7	-52 ± 7	-20 ± 3	-14 ± 5	-35 ± 5
93	-31 ± 6	-29 ± 3	-60 ± 8	-23 ± 4	-14 ± 2	-37 ± 6	-14 ± 2	-4 ± 0	-18 ± 2
94	-38 ± 8	-22 ± 4	-60 ± 9	-29 ± 2	-24 ± 3	-52 ± 3	-21 ± 2	-5 ± 2	-26 ± 3
95	-13 ± 3	0 ± 1	-13 ± 3	-7 ± 1	-10 ± 3	-17 ± 3	-5 ± 1	0 ± 1	-5 ± 0
137	-50 ± 1	-28 ± 6	-78 ± 28	-27 ± 1	-4 ± 1	-32 ± 2	-18 ± 2	-38 ± 3	-56 ± 2
140	-26 ± 2	-30 ± 2	-56 ± 1	-5 ± 3	-24 ± 4	-29 ± 6	-11 ± 1	-18 ± 7	-29 ± 4
145	-14 ± 4	-3 ± 2	-17 ± 2	-19 ± 8	-9 ± 7	-28 ± 9	-21 ± 4	-23 ± 4	-44 ± 8
150	-38 ± 3	-20 ± 3	-58 ± 6	-15 ± 3	-29 ± 7	-44 ± 9	-13 ± 1	-22 ± 5	-35 ± 4
168	-10 ± 2	-1 ± 1	-11 ± 5	-9 ± 1	-24 ± 3	-33 ± 3	-9 ± 0	-4 ± 2	-13 ± 3
175	-51 ± 9	-30 ± 8	-81 ± 15	-18 ± 1	-17 ± 3	-35 ± 1	-25 ± 4	-23 ± 11	-47 ± 6
177	-29 ± 6	-10 ± 6	-39 ± 6	-30 ± 7	-28 ± 12	-58 ± 9	-10 ± 2	-13 ± 15	-23 ± 10

[a] The data were averaged from the last 40 ns in three independent MD runs. ΔE_{elec}: electrostatic energy. ΔE_{vdW}: van der Waals. $\Delta G_{non\text{-}bond}$: the non-bond binding. $\Delta G_{non\text{-}bond} = \Delta E_{elec} + \Delta E_{vdW}$.

Table S7. The averaged non-bond binding energy between the substituted site and water molecules.[a]

Amino acid Position	Non-beneficial (kcal/mol)			Beneficial group 1 (kcal/mol)			Beneficial group 2 (kcal/mol)		
	ΔE_{vdW}	ΔE_{elec}	$\Delta G_{non\text{-}bond}$	ΔE_{vdW}	ΔE_{elec}	$\Delta G_{non\text{-}bond}$	ΔE_{vdW}	ΔE_{elec}	$\Delta G_{non\text{-}bond}$
4	-8 ± 2	-12 ± 5	-19 ± 1	2 ± 1	-29 ± 3	-27 ± 2	0 ± 2	-20 ± 12	-20 ± 10
12	-0 ± 2	-13 ± 10	-12 ± 2	2 ± 2	-32 ± 15	-30 ± 6	2 ± 1	-26 ± 7	-24 ± 7
14	-2 ± 1	-3 ± 1	-5 ± 1	4 ± 3	-40 ± 21	-37 ± 12	3 ± 2	-51 ± 29	-47 ± 21
15	-9 ± 3	-25 ± 4	-34 ± 7	3 ± 1	-36 ± 11	-33 ± 8	0 ± 2	-21 ± 5	-22 ± 5
17	-7 ± 1	-26 ± 11	-33 ± 6	-10 ± 2	-16 ± 7	-26 ± 2	0 ± 1	-39 ± 9	-39 ± 4
93	2 ± 2	-49 ± 7	-47 ± 6	0 ± 2	-23 ± 11	-24 ± 7	-1 ± 0	-5 ± 6	-7 ± 3
94	-9 ± 1	-20 ± 8	-30 ± 8	-7 ± 2	-7 ± 2	-14 ± 2	-7 ± 2	-3 ± 6	-10 ± 2
95	-3 ± 1	-0 ± 0	-3 ± 0	1 ± 0	-25 ± 3	-24 ± 7	0 ± 2	-11 ± 12	-11 ± 2
137	-8 ± 0	-4 ± 1	-12 ± 4	-4 ± 1	-1 ± 1	-4 ± 2	-2 ± 1	-15 ± 3	-17 ±1
140	3 ± 1	-44 ± 4	-41 ± 2	3 ± 1	-25 ±2	-22 ± 5	2 ± 2	-23 ± 11	-21 ± 9
145	-8 ± 1	-9 ± 9	-16 ± 1	-10 ± 3	-20 ± 11	-29 ± 7	1 ± 2	-71 ± 15	-70 ± 13
150	-10 ± 1	-37 ± 5	-47 ± 6	3 ± 2	-59 ± 11	-56 ± 7	3 ± 2	-49 ± 4	-46 ± 2
168	-5 ± 1	-3 ± 1	-8 ± 4	3 ± 1	-46 ± 4	-43 ± 3	-1 ± 1	-8 ± 6	-10 ± 3
175	-8 ± 3	-32 ± 8	-40 ± 5	2 ± 2	-45 ± 6	-42 ± 3	-2 ± 3	-37 ± 7	-39 ± 1
177	-3 ± 3	-18 ± 6	-21 ± 3	1 ± 2	-42 ± 18	-40 ± 8	0 ± 2	-30 ± 13	-29 ± 14

[a] The data were averaged from the last 40 ns in three independent MD runs. ΔE_{elec}: electrostatic energy. ΔE_{vdW}: van der Waals. $\Delta G_{non\text{-}bond}$: the non-bond binding. $\Delta G_{non\text{-}bond} = \Delta E_{elec} + \Delta E_{vdW}$.

Table S8. Analysis of 1267 polar substitution that all type of amino acid substitute to polar residue towards OSs resistance in BSLA-SSM library.[a]

The fraction of substitutions	% (variants)	Beneficial	Unchanged	Decreased	Inactive
All to polar	DMSO	12.2% (154/1267)	57.9% (734/1267)	14.8% (187/1267)	15.2% (192/1267)
	DOX	3.7% (47/1267)	65.2% (873/1267)	12.8% (162/1267)	18.3% (232/1267)
	TFE	6.6% (84/1267)	59.8% (842/1267)	12.0% (425/1267)	21.5% (273/1267)

[a] 22% (v/v) DOX, 60% (v/v) DMSO, and 12% (v/v) TFE were used. Amino acid is classified as follows: Aromatic: F, Y, W; Aliphatic: A, V, L, I, G; Polar: C, M, P, S, T, N, Q; Charged: D, E, K, H, R.

Table S9. Analysis of the 364 non-polar substitutions that polar amino acid substitute to non-polar residue towards OSs resistance in BSLA-SSM library.[a]

The fraction of substitutions % (variants)		Beneficial	Unchanged	Decreased	Inactive
polar to non-polar	DMSO	9.1% (33/364)	72.3% (296/364)	11.5% (68/364)	7.1% (26/364)
	DOX	6.3% (23/364)	79.1% (311/364)	6.0% (53/364)	8.5% (31/364)
	TFE	11.3% (41/364)	69.2% (293/364)	8.5% (71/364)	11.0% (40/364)

[a] 22% (v/v) DOX, 60% (v/v) DMSO, and 12% (v/v) TFE were used. Amino acid is classified as follows: Aromatic: F, Y, W; Aliphatic: A, V, L, I, G; Polar: C, M, P, S, T, N, Q; Charged: D, E, K, H, R.

Table S10. Analysis of the 896 surface polar substitutions that all type of amino acid substitute to polar residue towards OSs resistance in BSLA-SSM library.[a]

The fraction of substitutions	% (variants)	Beneficial	Unchanged	Decreased	Inactive
Surface residue to polar	DMSO	11.4% (102/896)	66.2% (593/896)	12.8% (115/896)	9.6% (86/896)
	DOX	4.0% (36/896)	75.1% (695/896)	9.9% (89/896)	10.9% (98/896)
	TFE	7.5% (67/896)	69.3% (621/896)	8.7% (78/896)	14.5% (130/896)

[a] 22% (v/v) DOX, 60% (v/v) DMSO, and 12% (v/v) TFE were used. Amino acid is classified as follows: Aromatic: F, Y, W, A; Aliphatic: A, V, L, I, G; Polar: C, M, P, S, T, N, Q; Charged: D, E, K, H, R.

Table S11. Analysis of the surface polar substitutions that different amino acid substitute to polar residue towards OSs resistance in BSLA-SSM library.[a]

The fraction of substitutions % (variants)		Beneficial	Unchanged	Decreased	Inactive
Polar to polar	DMSO	11.1% (33/301)	74.4% (224/301)	7.3% (22/301)	7.3% (22/301)
	DOX	4.0% (12/301)	83.1% (250/301)	4.3% (13/301)	8.6% (26/301)
	TFE	4.0% (12/301)	80.4% (242/301)	3.0% (9/301)	12.6% (38/301)
Aromatic to polar	DMSO	14.3% (12/84)	66.7% (56/84)	7.1% (6/84)	11.9% (10/84)
	DOX	4.8% (4/84)	75.0% (63/84)	8.3% (7/84)	11.9% (10/84)
	TFE	4.8% (4/84)	77.4% (65/84)	4.6% (3/84)	14.3% (12/84)
Aliphatic to polar	DMSO	14.0% (43/308)	60.4% (186/308)	17.2% (53/308)	8.4% (26/308)
	DOX	2.9% (9/308)	72.1% (222/308)	14.0% (43/308)	11.0% (34/308)
	TFE	4.9% (15/308)	69.5% (214/308)	7.1% (22/308)	18.5% (57/308)
Charged to polar	DMSO	6.9% (14/203)	62.6% (127/203)	16.7% (34/203)	13.8% (28/203)
	DOX	2.0% (4/203)	78.8% (160/203)	4.9% (10/203)	14.3% (29/203)
	TFE	7.4% (15/203)	74.4% (151/203)	2.0% (4/203)	16.3% (33/203)

[a] 22% (v/v) DOX, 60% (v/v) DMSO, and 12% (v/v) TFE were used. Amino acid is classified as follows: Aromatic: F, Y, W; Aliphatic: A, V, L, I, G; Polar: C, M, P, S, T, N, Q; Charged: D, E, K, H, R.

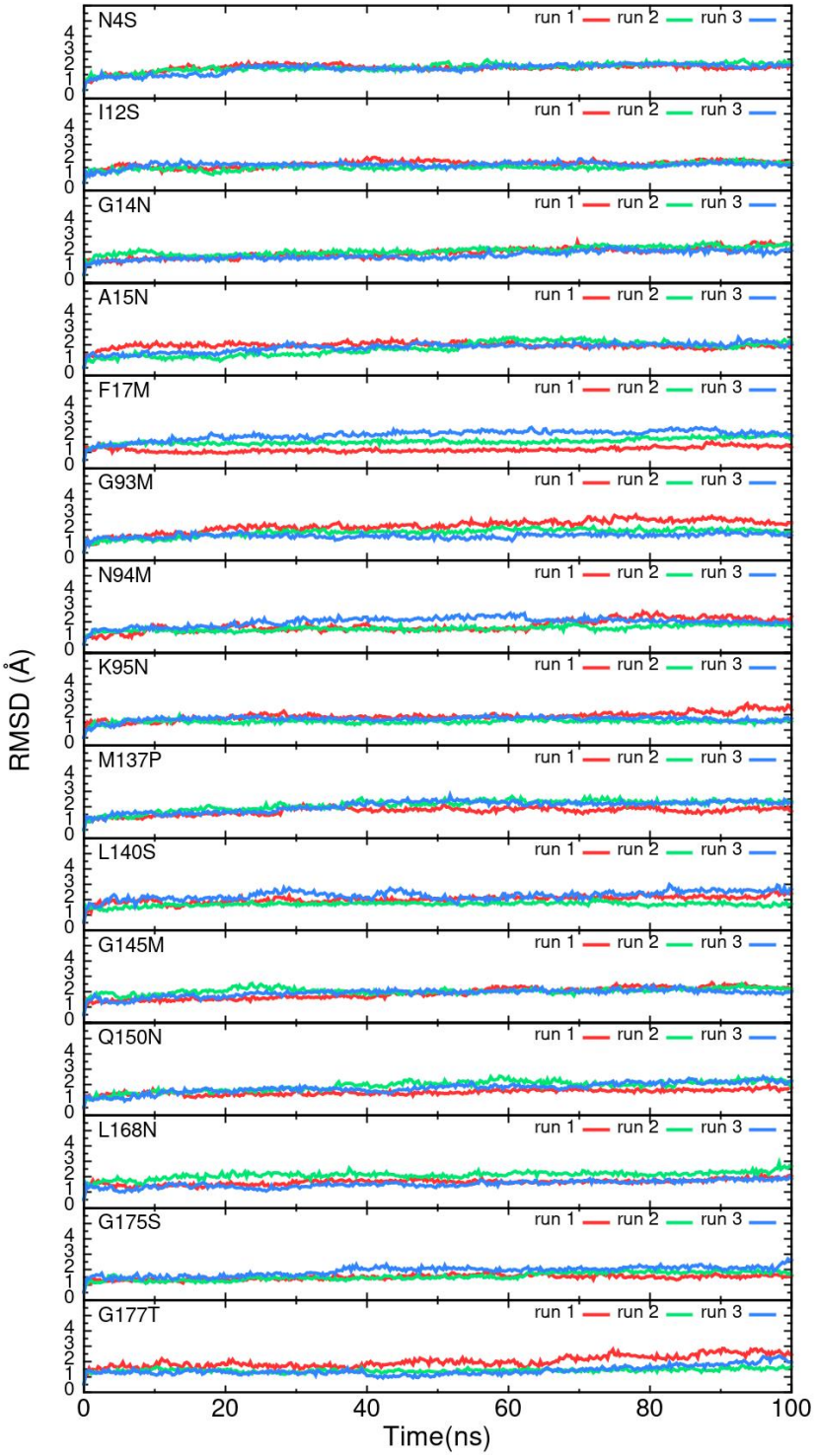

Figure S1. Root-mean-square deviation (RMSD) of the BSLA non-beneficial substitutions backbone with respect to the initial structure as a function of time in 60 % (v/v) DMSO. Three independent MD runs for each solvent are shown.

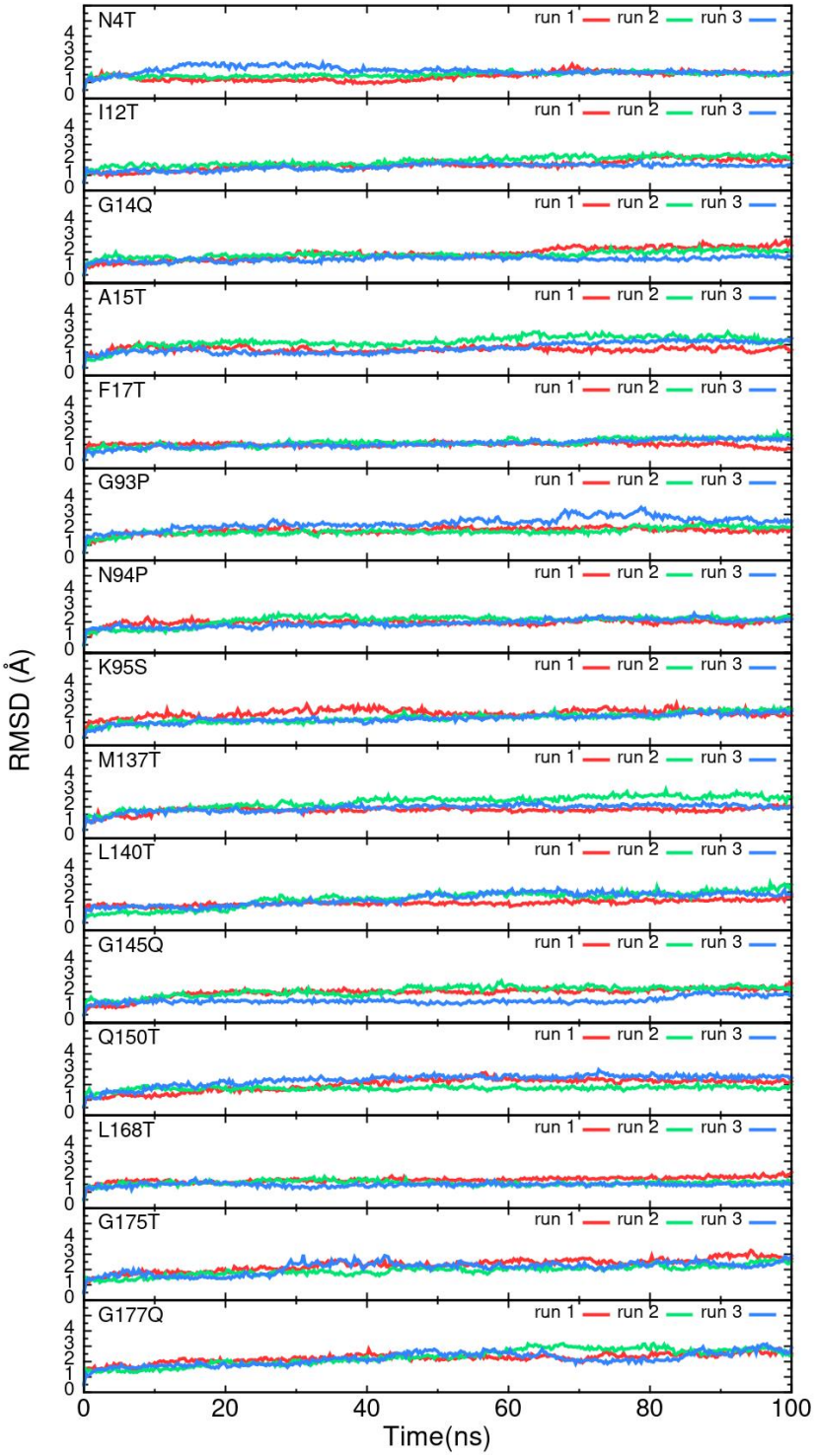

Figure S2. Root-mean-square deviation (RMSD) of the BSLA beneficial substitutions (group 1) backbone with respect to the initial structure as a function of time in 60 % (v/v) DMSO. Three independent MD runs for each solvent are shown.

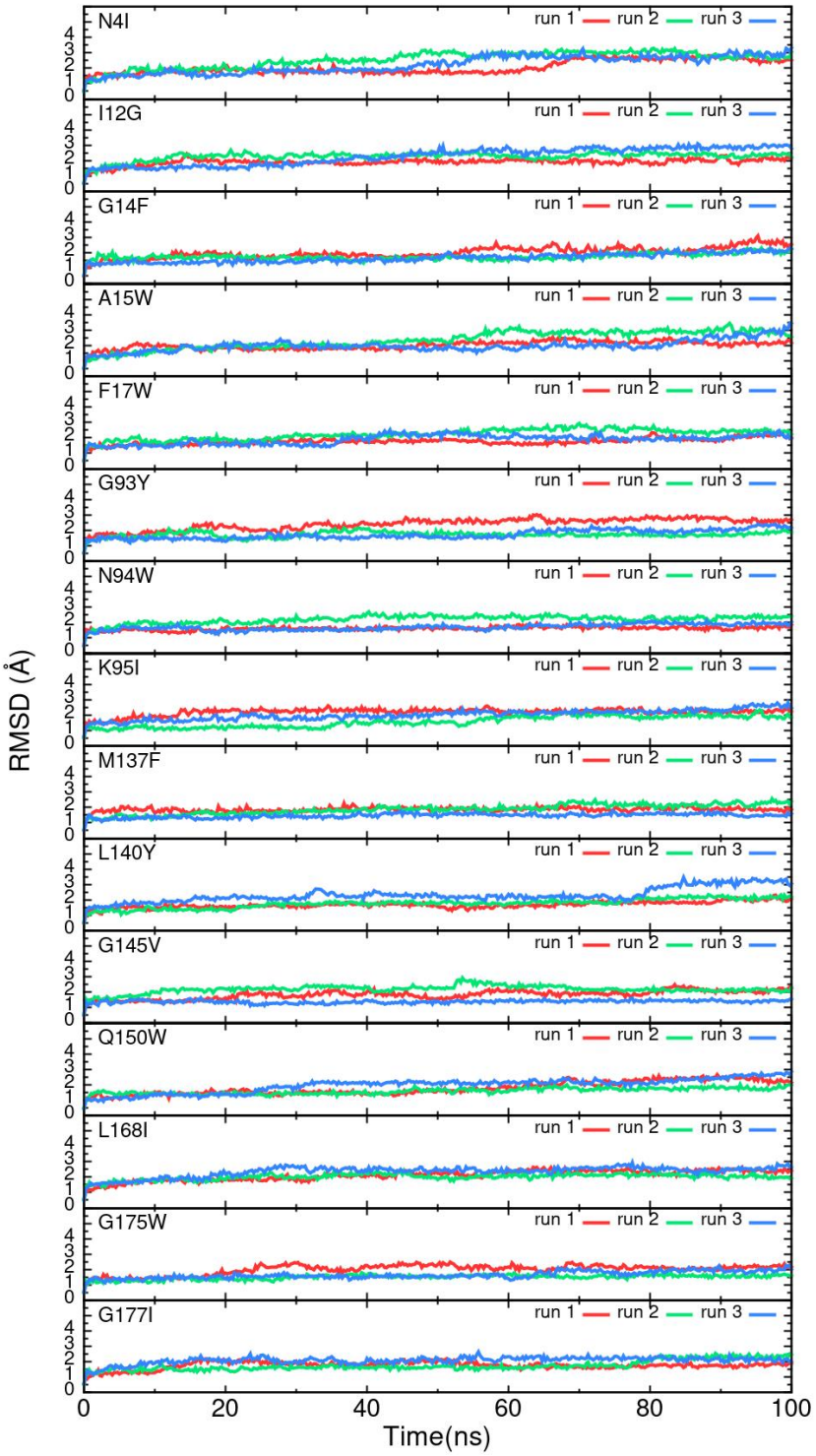

Figure S3. Root-mean-square deviation (RMSD) of the BSLA beneficial substitutions (group 2) backbone with respect to the initial structure as a function of time in 60 % (v/v) DMSO. Three independent MD runs for each solvent are shown.

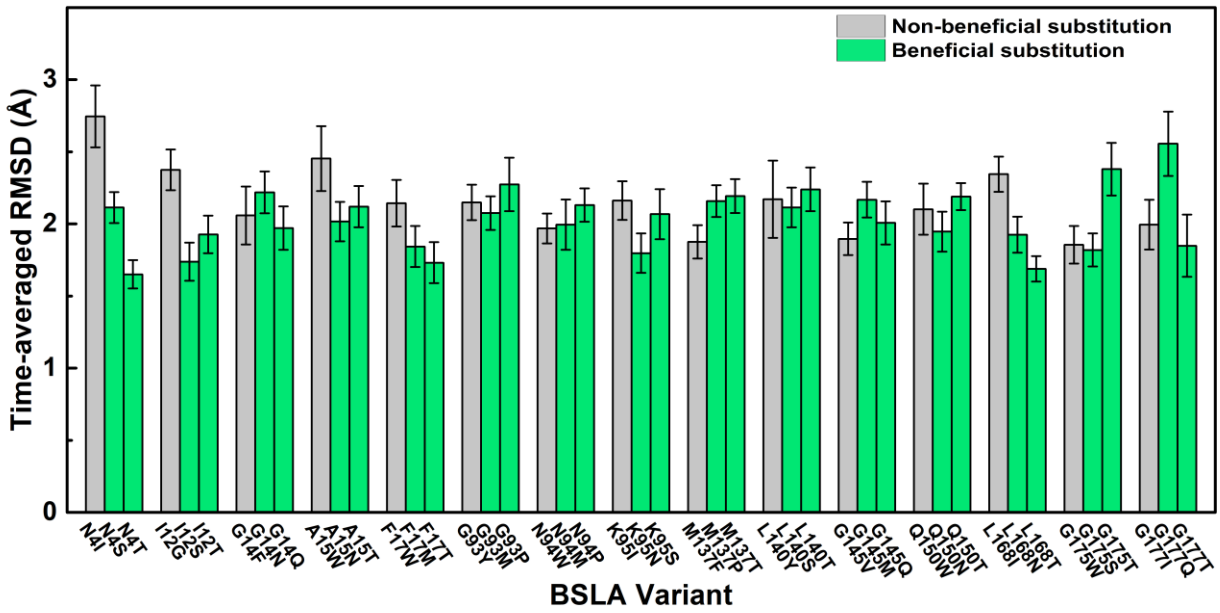

Figure S4. Time-average RMSD of BSLA non-beneficial and beneficial substitutions determined from the last 40 ns of simulations in 60 % (v/v) DMSO. Error bars describe the standard deviation from three independent MD runs.

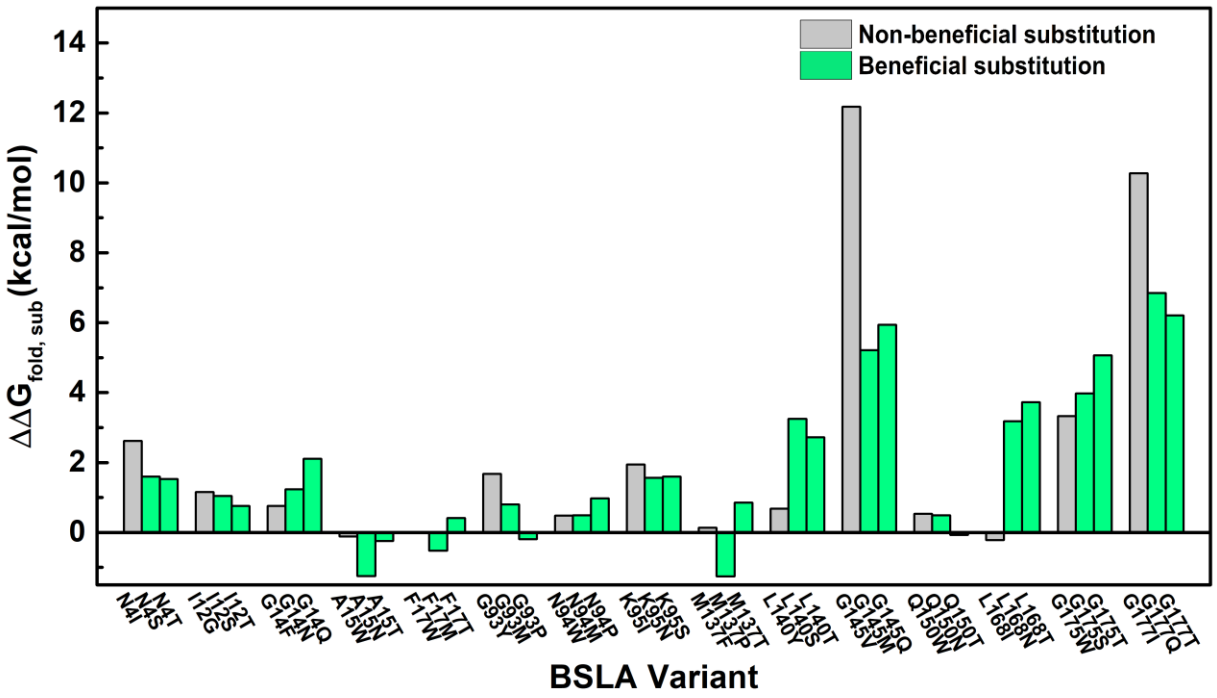

Figure S5. Thermodynamic stability ($\Delta\Delta G_{fold}$) of BSLA beneficial and non-beneficial substitutions. The relative folding free energies ($\Delta\Delta G_{fold} = \Delta G_{fold,sub} - \Delta G_{fold,wt}$) were computed using FoldX 4 [7] employing YASARA Plugin [8] in YASARA Structure version 17.4.17 [9] as our previous reported.[10] The larger the $\Delta\Delta G_{fold}$ negative values, the higher the stability.

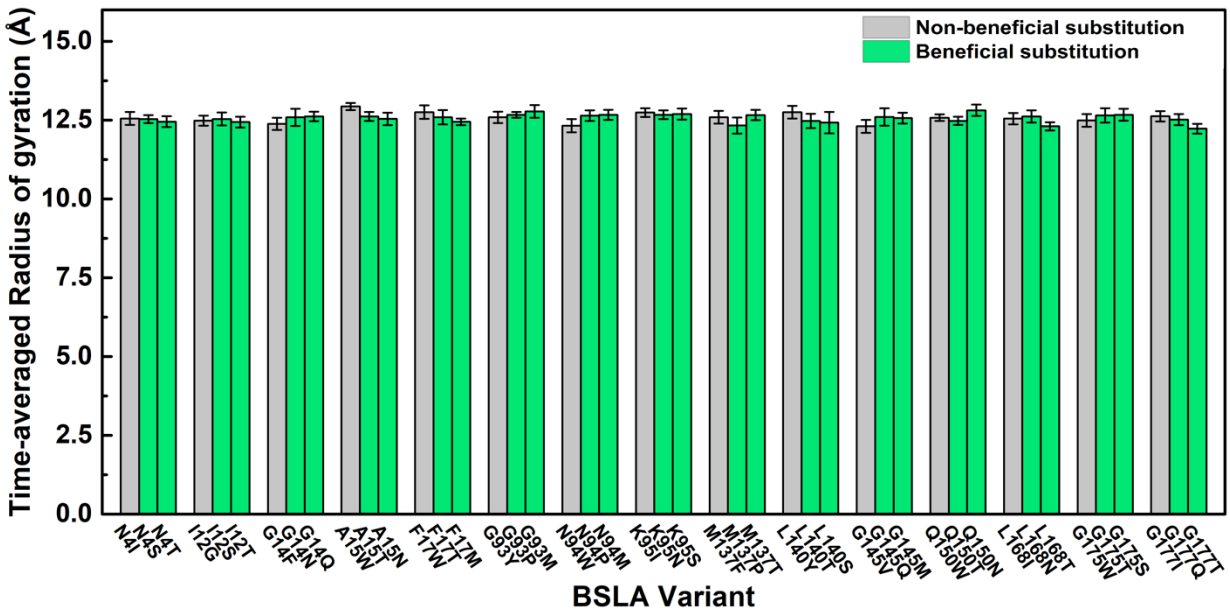

Figure S6. The time-averaged radius of gyration (R_g) of BSLA non-beneficial and beneficial substitutions in 60 % (v/v) DMSO, the time-averaged R_g was calculated from the last 40 ns of the MD simulations. Error bars show the standard deviation from three independent MD runs.

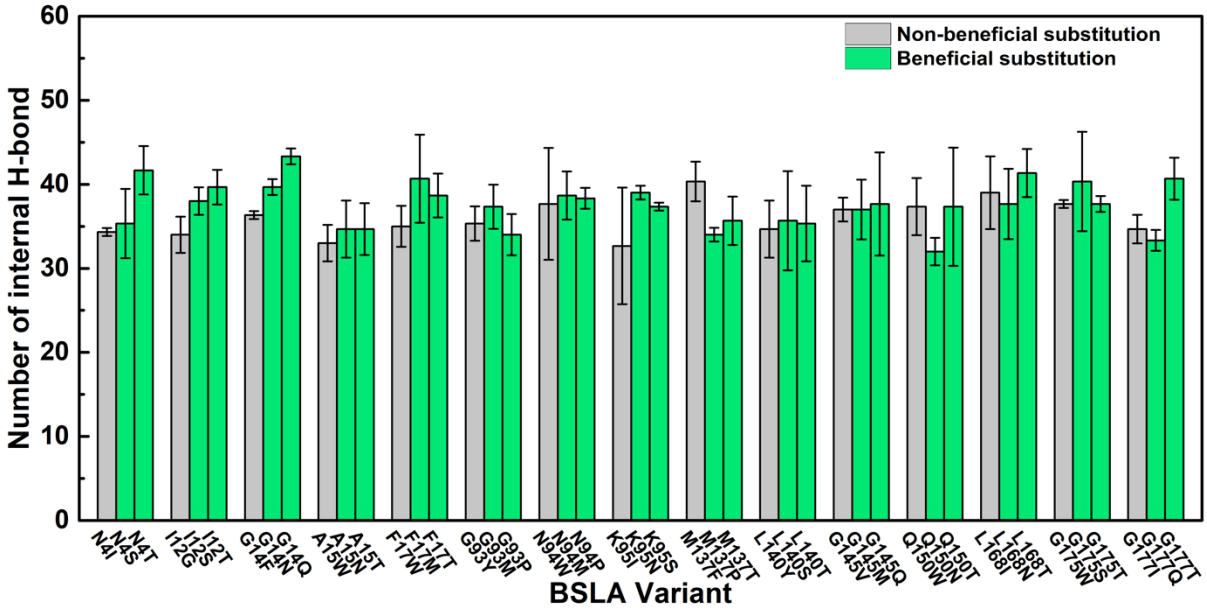

Figure S7. The number of internal hydrogen bonds with > 95% occupancy in BSLA beneficial and non-beneficial substitutions in 60 % (v/v) DMSO. All the data were calculated from the last 40 ns of the simulation. Error bars show the standard deviation from three independent MD runs. Geometric cut off for evaluation of hydrogen bond distance 3.5 Å and angle 30° were used.

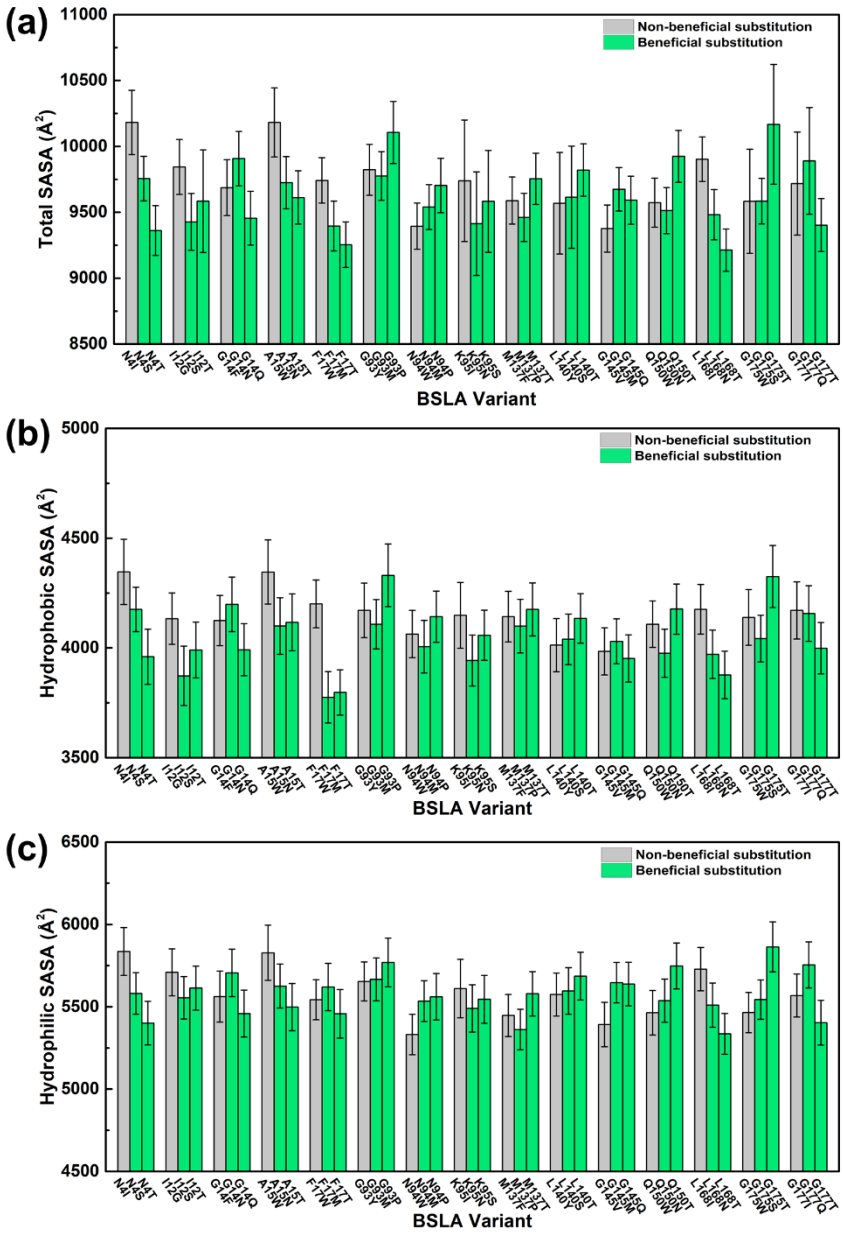

Figure S8. The time-averaged (**a**) total (**b**) hydrophobic (**c**) hydrophilic SASA of BSLA beneficial and non-beneficial substitutions in 60 % (v/v) DMSO. The average of SASA is computed based on the last 40 ns of each simulation. Error bars show the standard deviation from three independent MD runs for each variant. Here, SASA refers to the surface area of BSLA, which is accessible to water molecules and DMSO molecules calculated using a probe of radius 1.4 Å. The cut off -0.2 to 0.2 was used for hydrophobic and hydrophilic SASA calculations.[11]

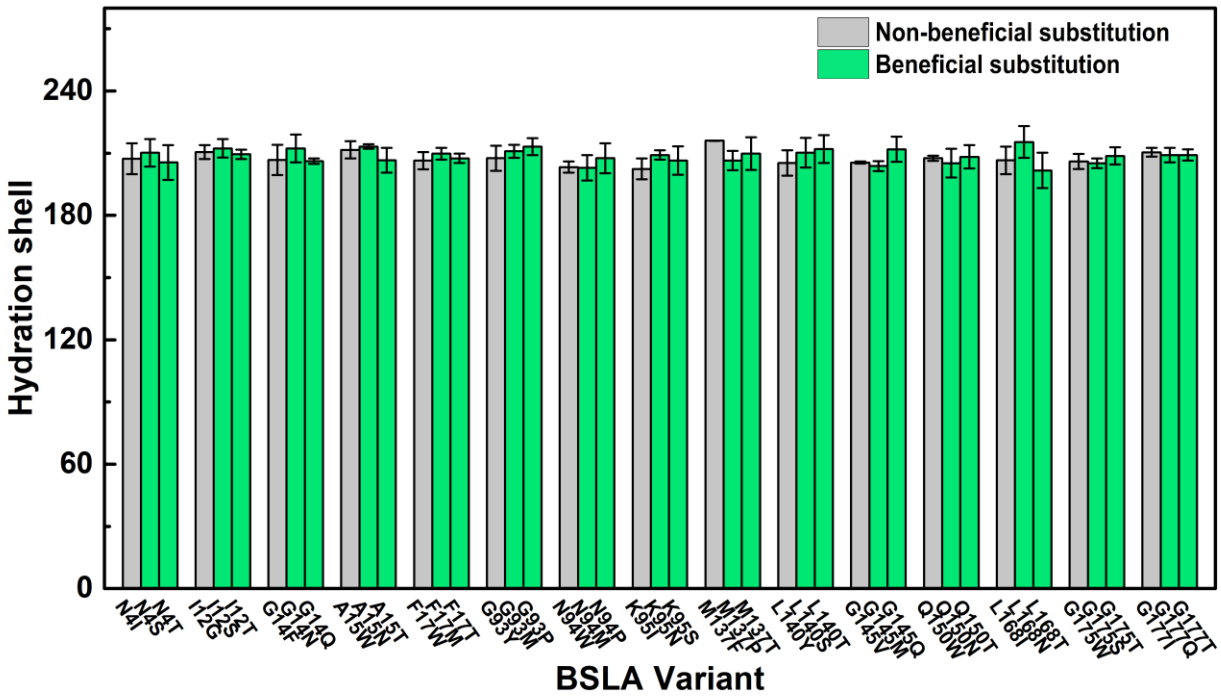

Figure S9. Hydration shell of BSLA beneficial and non-beneficial substitutions in 60 % (v/v) DMSO during MD simulations. Water molecules whose O atom is within 3.5 Å distance cut-off of any non-hydrogen atom of BSLA were described as the first hydration shell. The data of the hydration shell was averaged from three independent simulation runs.

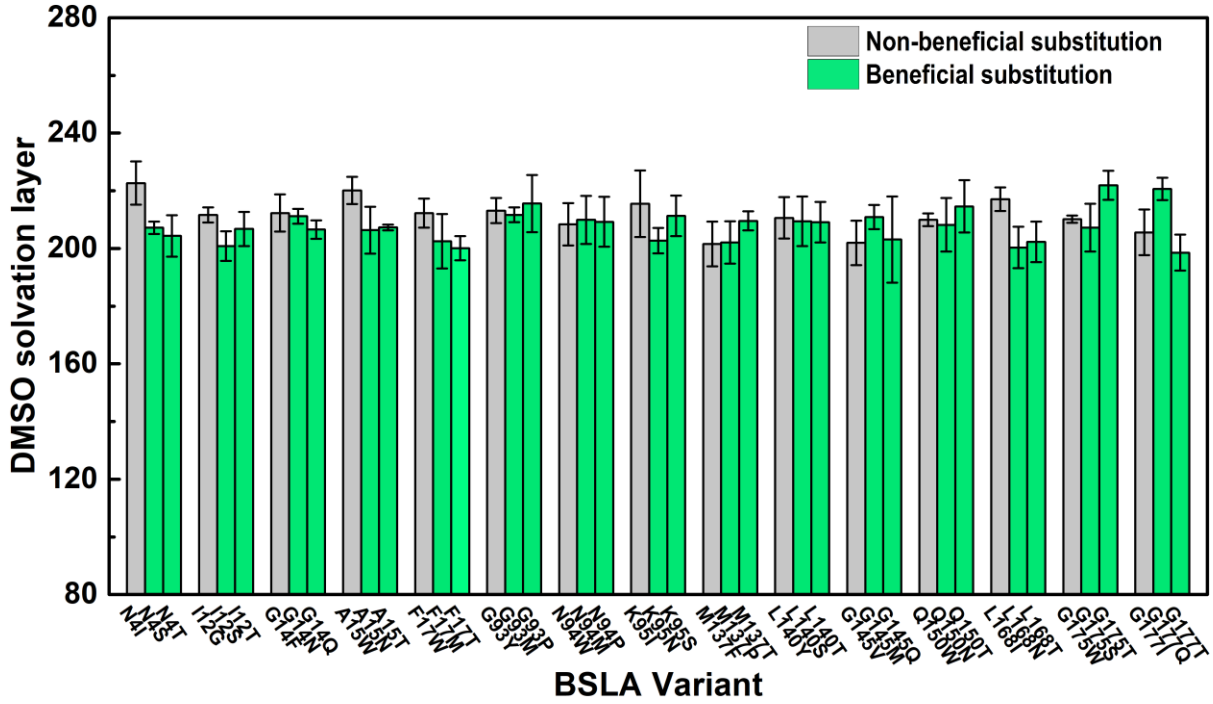

Figure S10. DMSO solvation layer of BSLA the non-beneficial and beneficial substitution in 60 % (v/v) DMSO during MD simulations**.** A similar definition with the hydrogen level is also defined for the organic solvent layer. A 6.8 Å cut-off was employed for DMSO as a previous study.[1] The data of the DMSO layer was averaged from three independent simulation runs

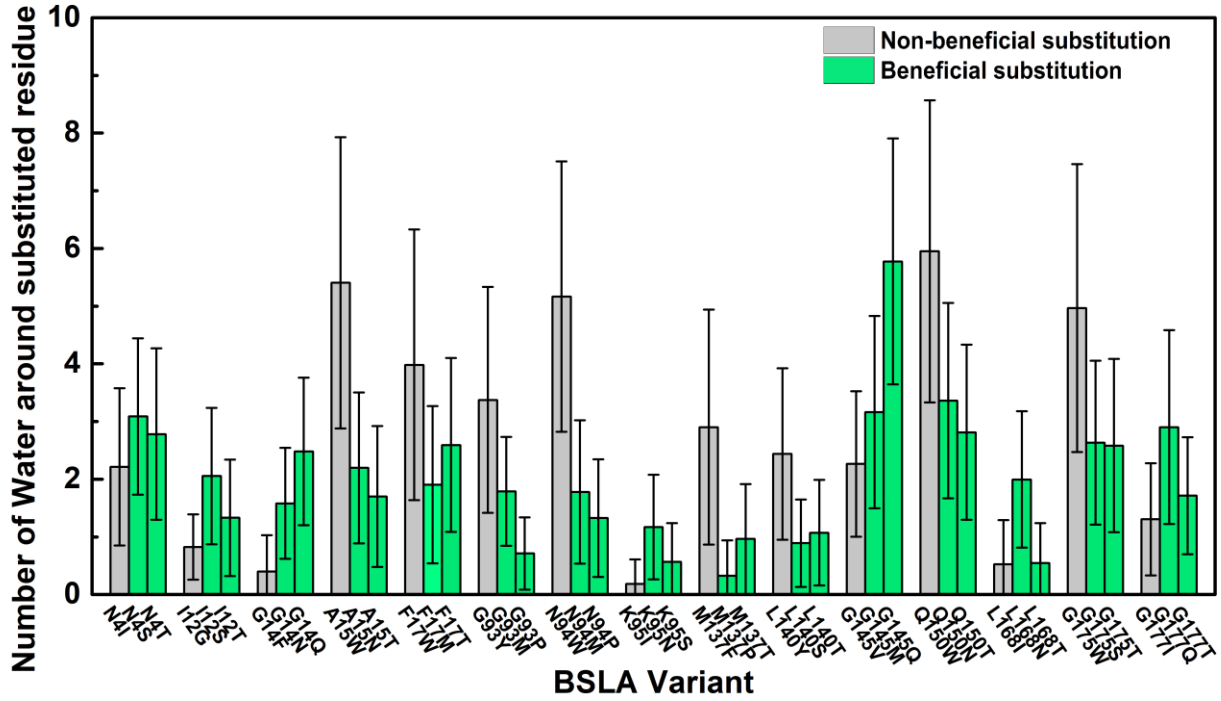

Figure S11. The average number of water molecules around the BSLA substituted residue during the MD simulations in 60 % (v/v) DMSO. The number of Water molecules was averaged over the last 40 ns from three independent MD runs.

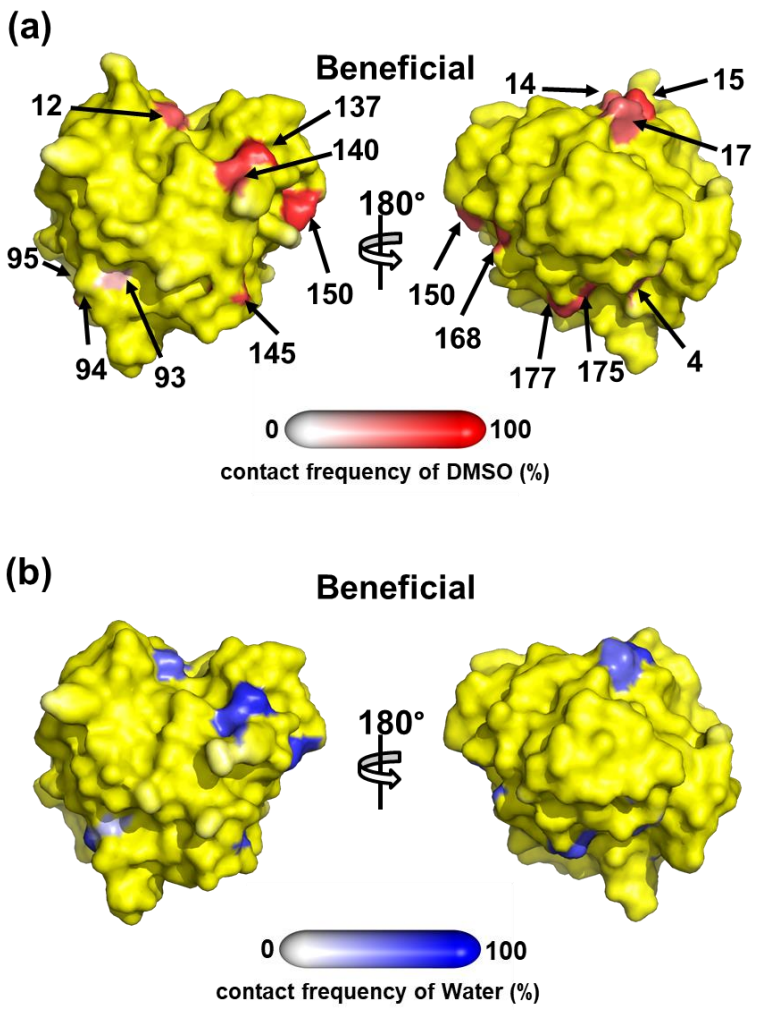

Figure S12. Contacts frequency of substituted sites between the BSLA beneficial substitution (group 2) and (**a**) water, (**b**) DMSO molecule in 60 % (v/v) DMSO, respectively. Residue-water/DMSO contact was defined as residue-water/DMSO molecule distance being 2.5 Å or less.[1] Contact frequency was calculated over the last 40 ns from three independent MD runs. The ramp was colored from white to blue/red to indicate the change of residue-water/DMSO contact frequency from low to high. Specific substituted sites are labeled with amino acid position number. Except for the substituted sites, the rest surface is colored with yellow. Front-side (rotated by 180°) views are shown to give a complete view of the BSLA substitutions. Each view of BSLA has the same orientation.

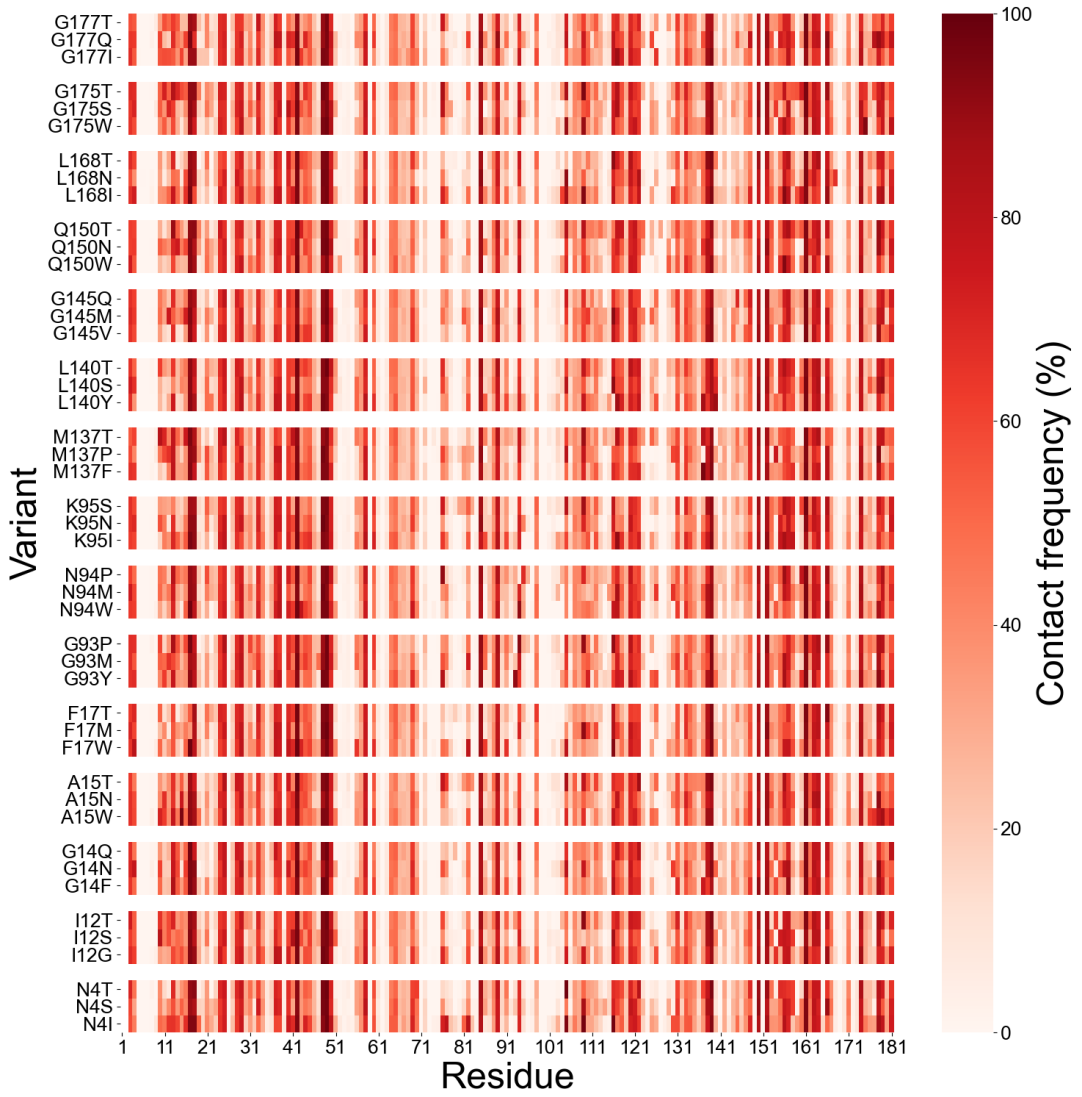

Figure S13. Contacts frequency between each BSLA residue and DMSO towards non-beneficial and beneficial substitutions in 60 % (v/v) DMSO. The cut-off 2.5 Å was applied to define the residue-DMSO contact.

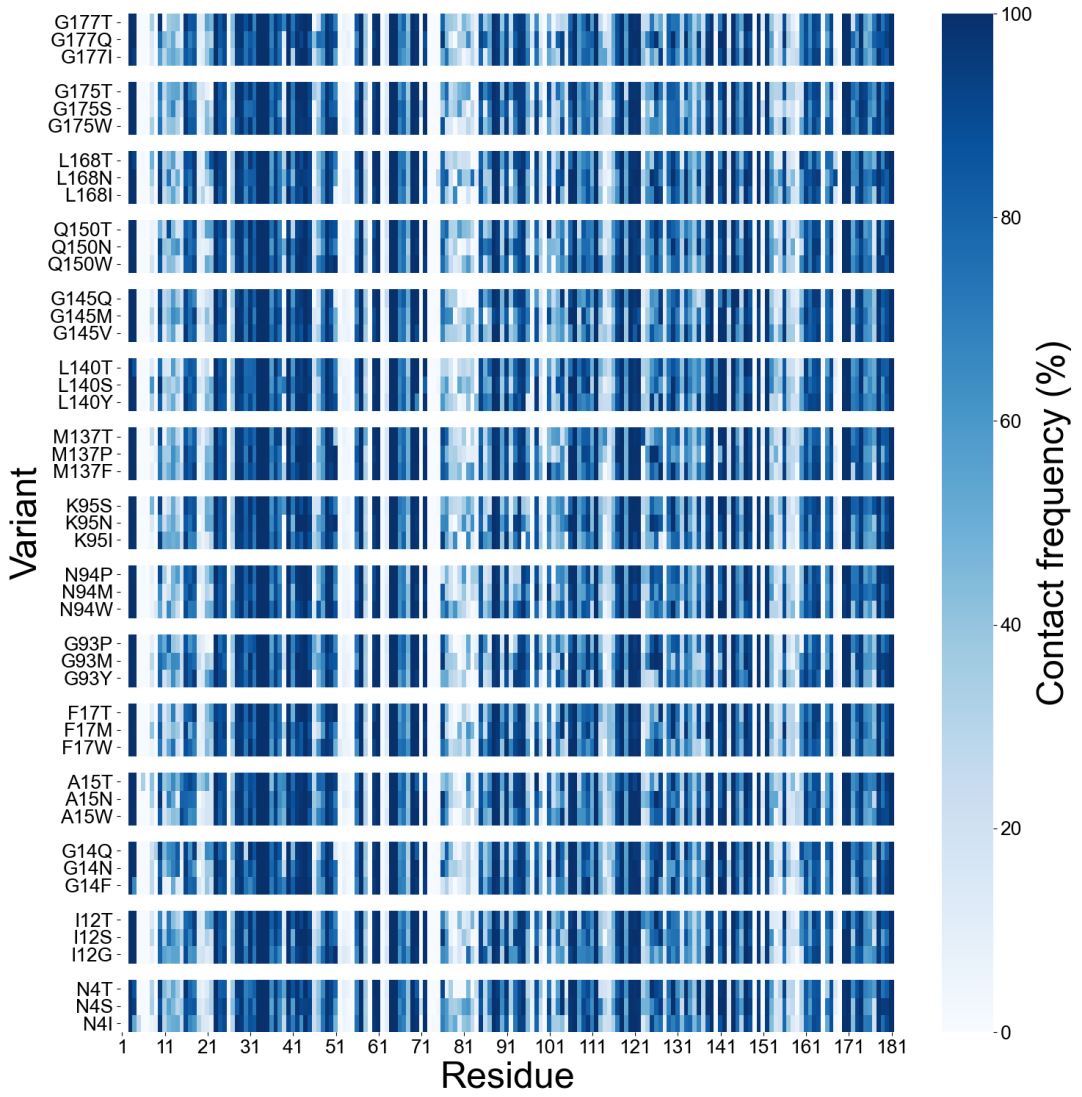

Figure S14. Contacts frequency between each BSLA residue and water towards non-beneficial and beneficial substitutions in 60 % (v/v) DMSO. The cut-off 2.5 Å was applied to define the residue-water contact.

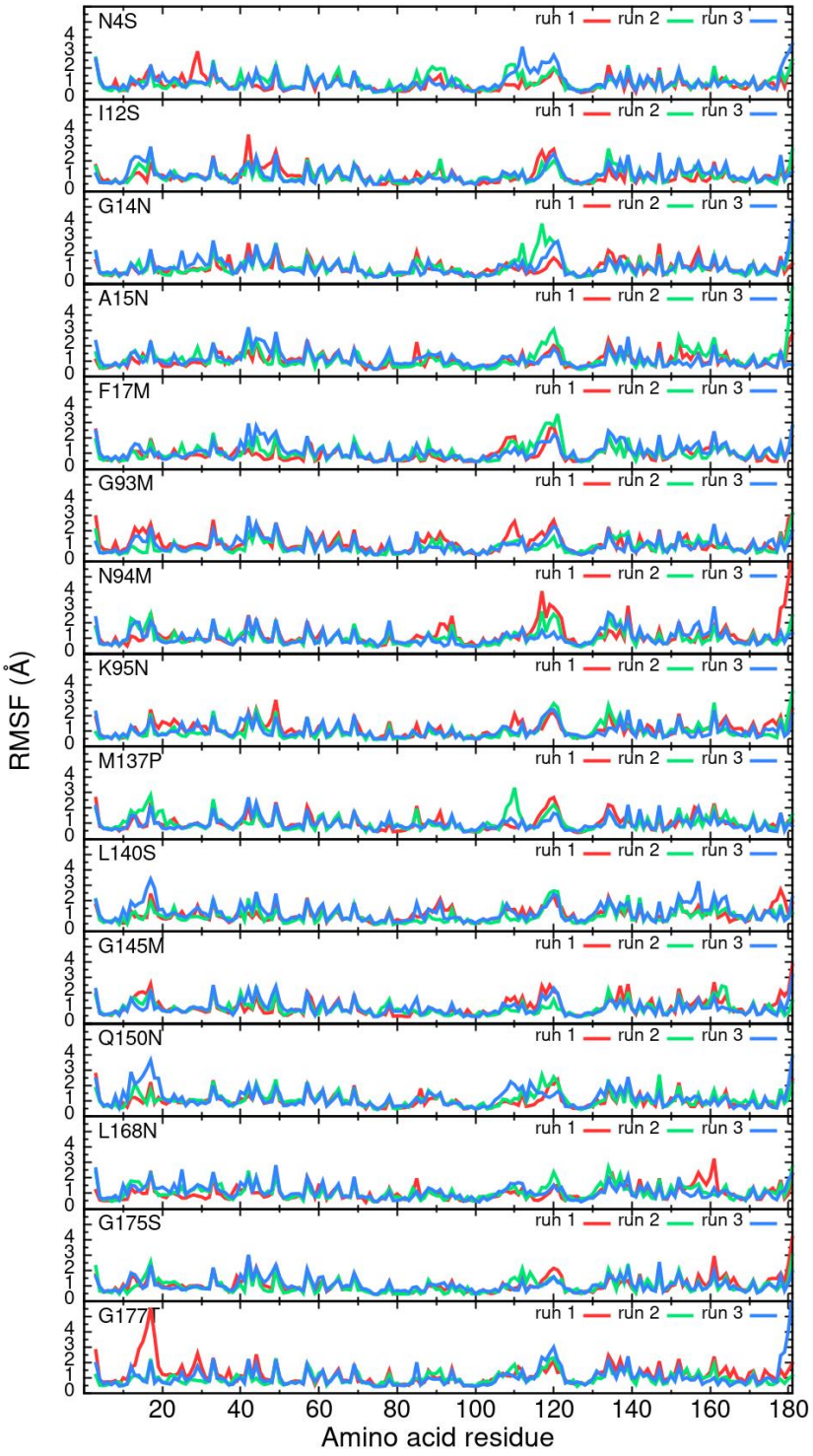

Figure S15. RMSF of each residue of BSLA non-beneficial substitutions determined from the last 40 ns of MD simulations in 60 % (v/v) DMSO. Three independent MD runs are shown.

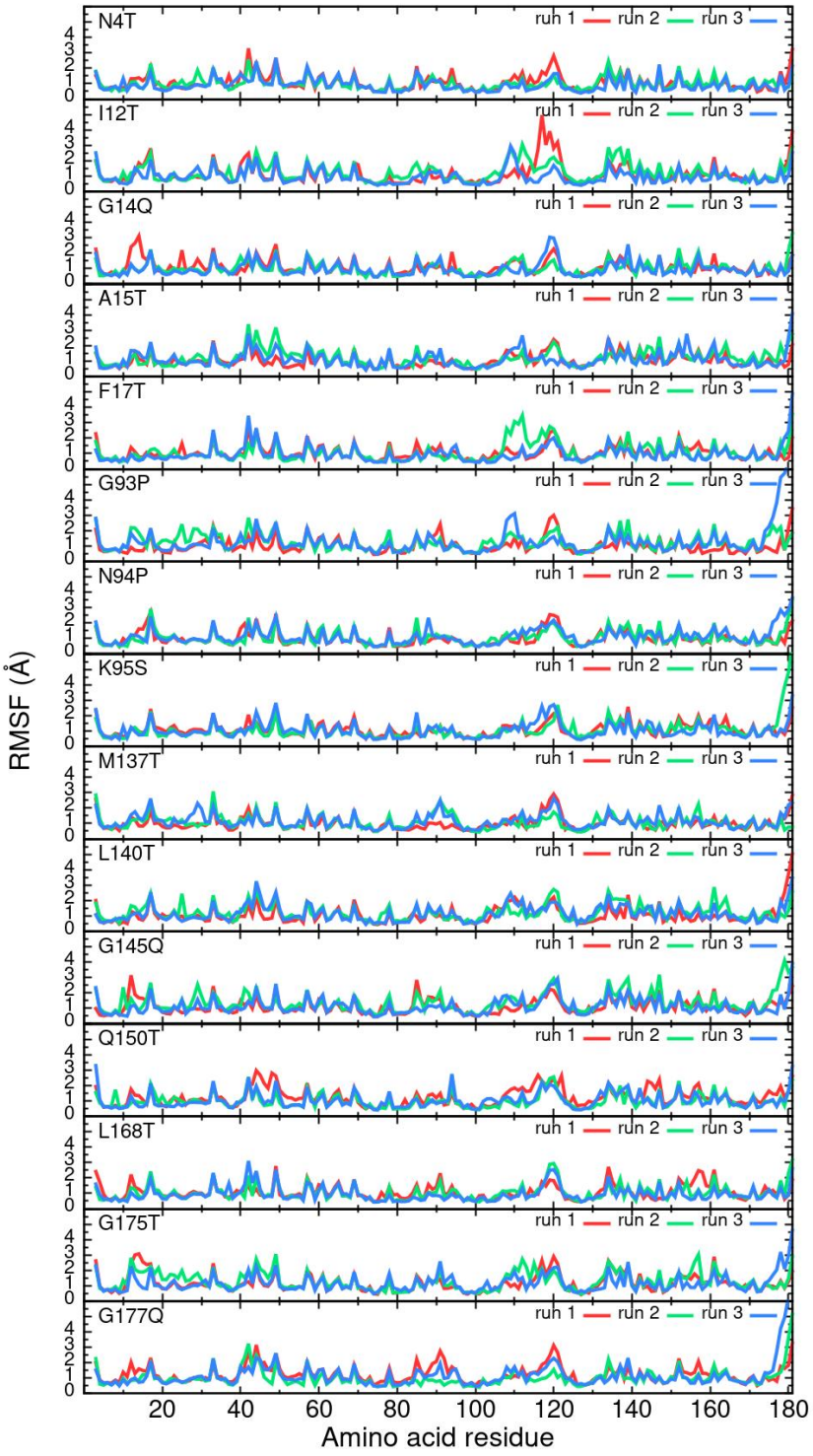

Figure S16. RMSF of each residue of BSLA beneficial substitutions (group 1) determined from the last 40 ns of MD simulations in 60 % (v/v) DMSO . Three independent MD runs are shown.

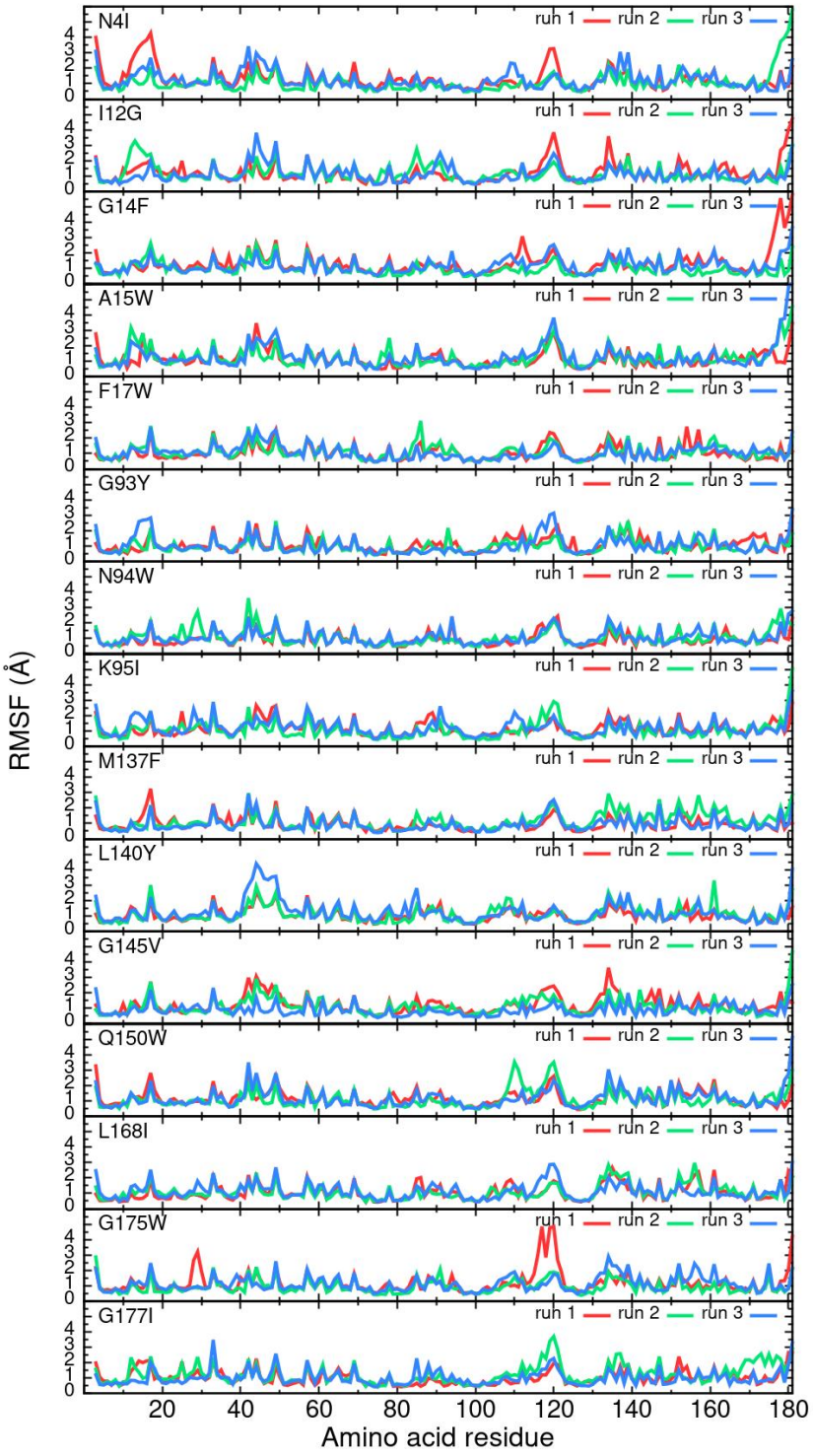

Figure S17. RMSF of each residue of BSLA beneficial substitutions (group 2) determined from the last 40 ns of MD simulations in 60 % (v/v) DMSO . Three independent MD runs are shown.

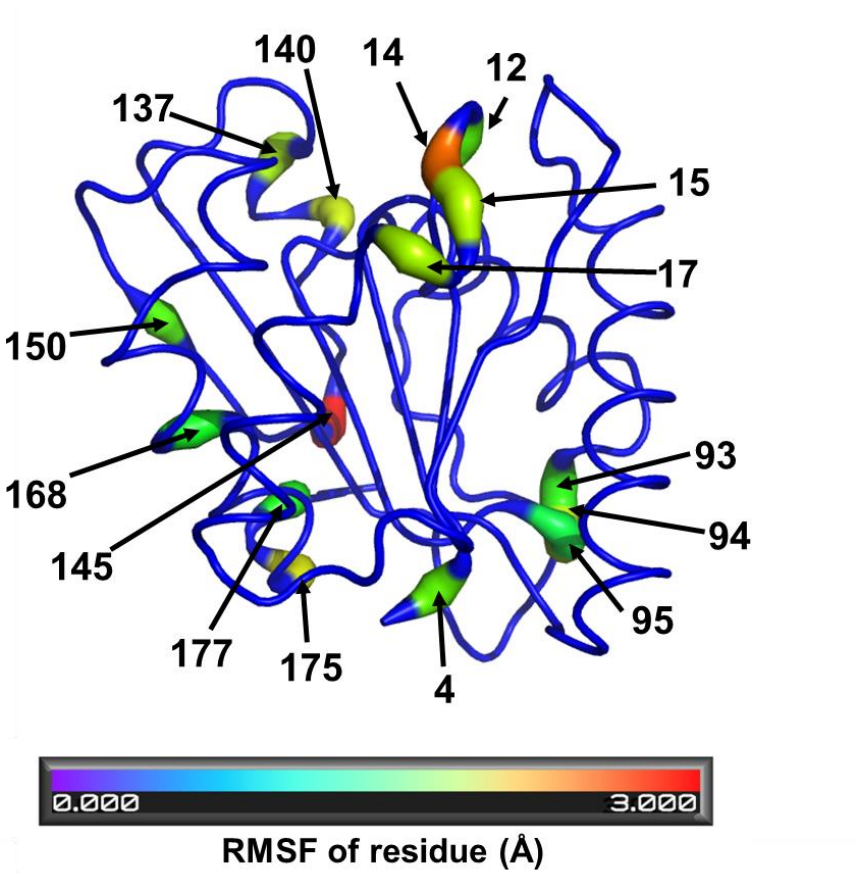

Figure S18. The RMSF of the substituted residue of BSLA beneficial substitutions (group 2) in 60 % (v/v) DMSO during MD simulations. The RMSF of substituted residue was averaged over the last 40 ns of three independent simulations.

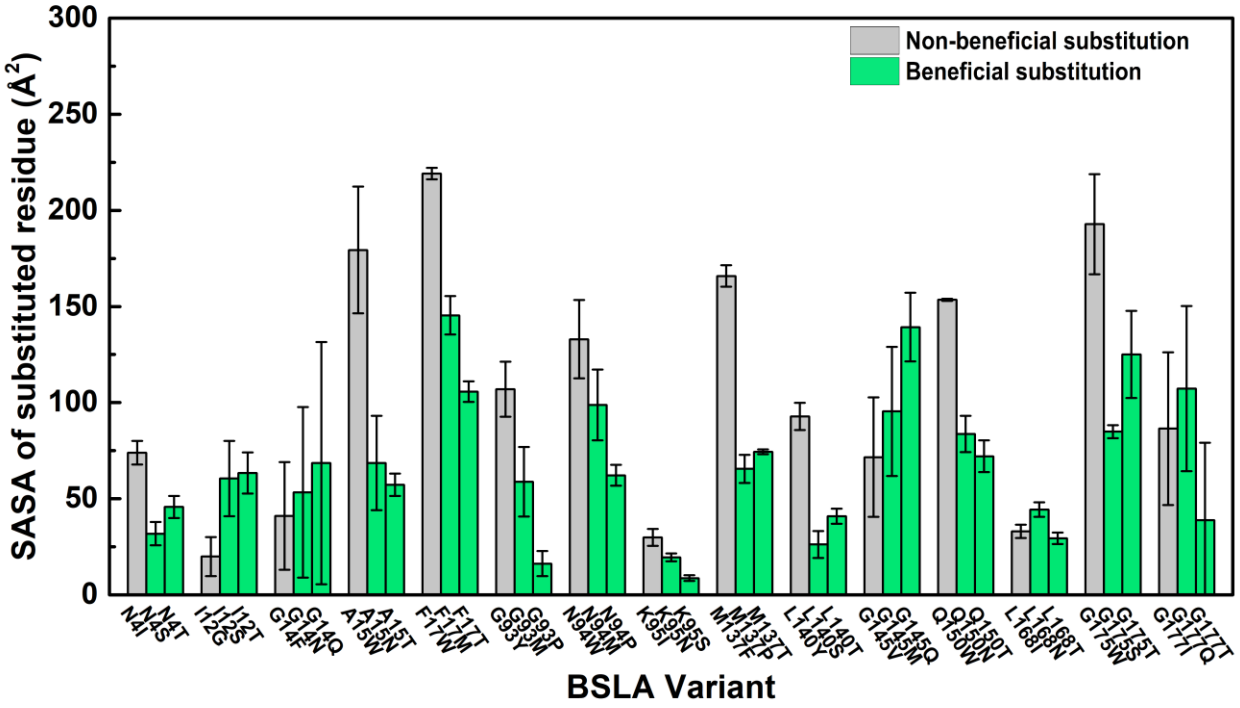

Figure S19. The SASA of the substituted residue of BSLA beneficial and non-beneficial substitutions in 60 % (v/v) DMSO during MD simulations. The SASA of substituted residue was averaged over the last 40 ns of three independent simulations.

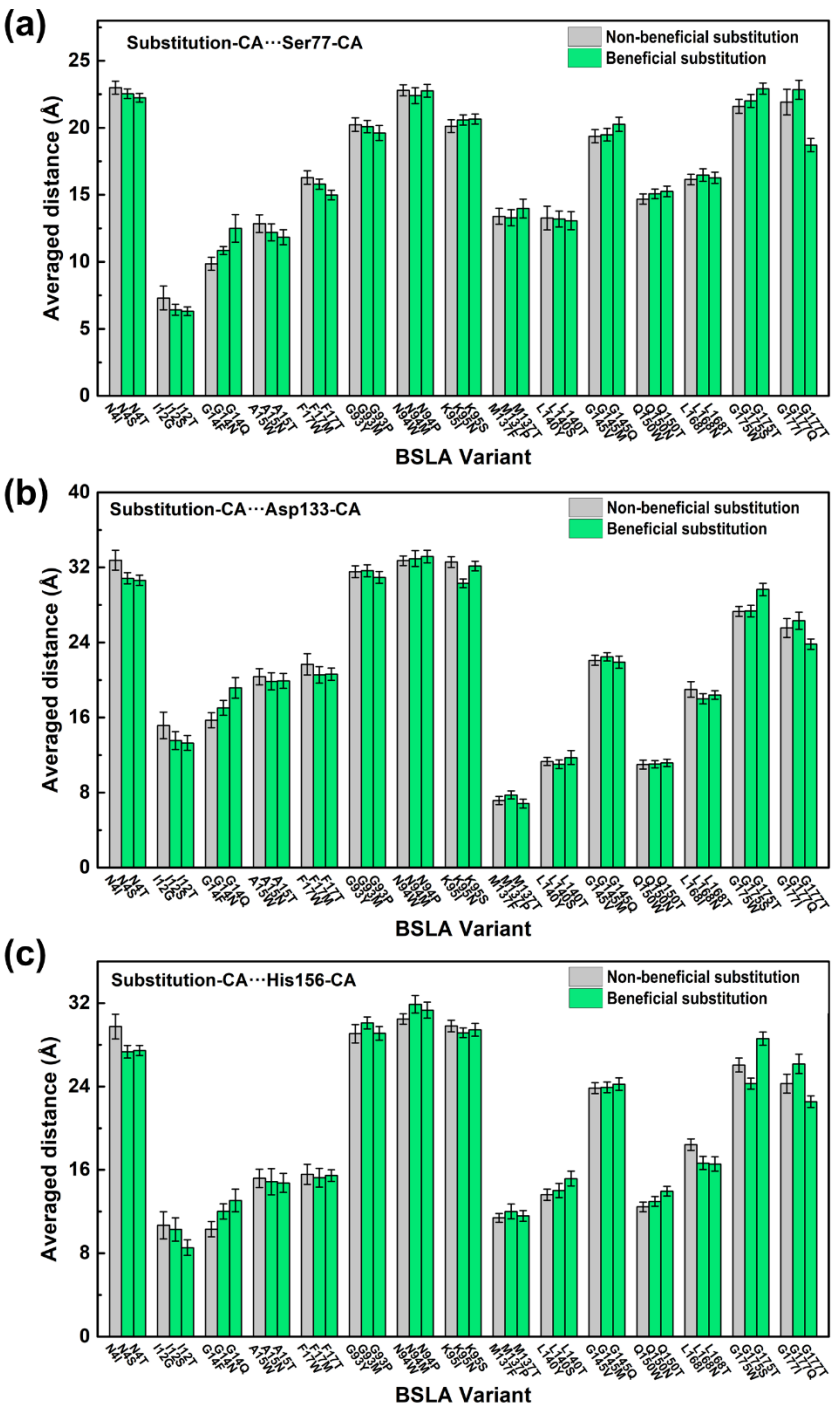

Figure S20. Averaged distance between substituted residue and the catalytic triad (**a**) Ser77, (**b**) Asp133, (**c**) His156 of BSLA beneficial and non-beneficial substitutions in 60 % (v/v) DMSO. The internal-atomic (C_α atom) distance (Å) is defined as the distance between substituted residue and the catalytic triad and averaged over the last 40 ns of three independent simulations.

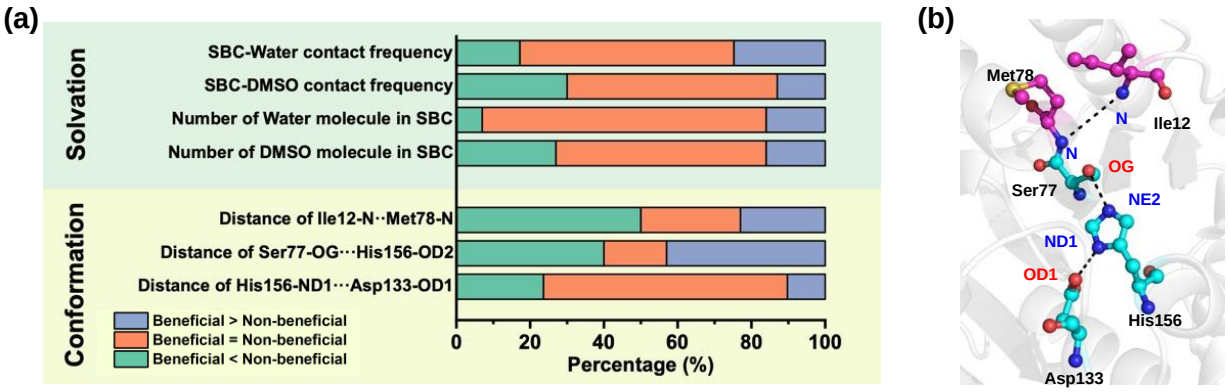

Figure S21. Conformational and solvation change in the substrate binding cleft. (**a**) The conformational change in the substrate binding cleft (SBC) described by calculating the averaged internal-atomic distance between the catalytic triad and oxyanion hole of BSLA variants. The DMSO/water solvation in SBC was calculated as previously reported, respectively. Representative structures of the catalytic triad and oxyanion hole were taken from BSLA WT (PDB ID: 1i6w,[3] Chain A). (**b**) The catalytic triad (Ser77, His156, Asp133) and oxyanion hole (Ile12, Met78) are shown as ball-and-stick with carbon (cyan/purple), oxygen (red), and nitrogen (blue). The black dashed line indicates the distance between two atoms.

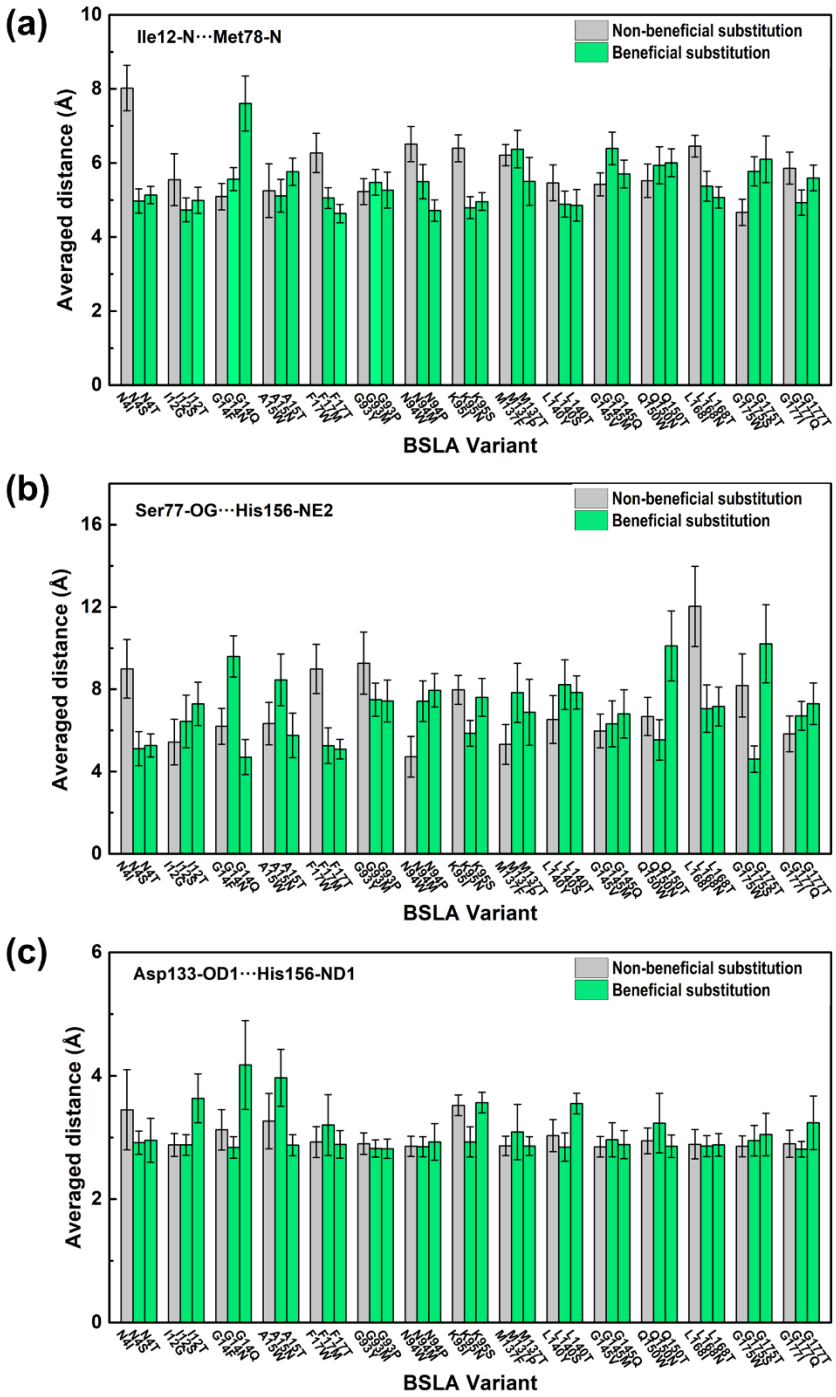

Figure S22. The averaged internal-atomic distance between the catalytic triad (Ser77, His156, Asp133) and oxyanion hole (Ile12, Met78) of BSLA beneficial and non-beneficial substitutions: (**a**) Ile12-N···Met78-N. (**b**) Ser77-OG···His156-NE2 and (**c**) His156-ND1···Asp133-OD1.

.

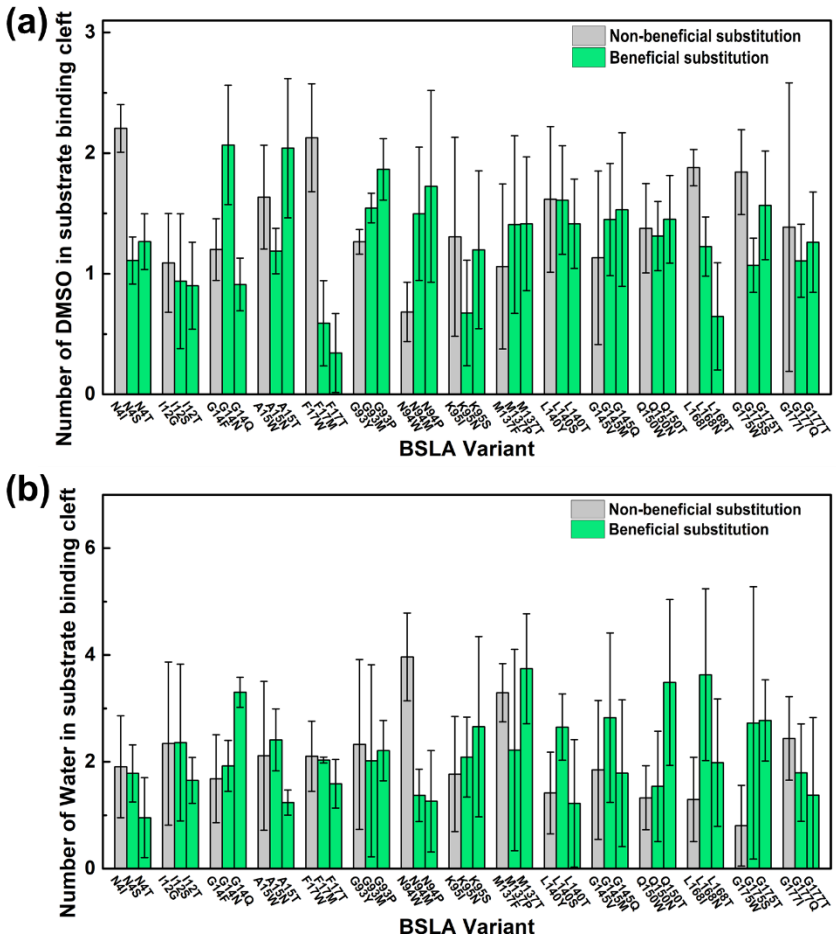

Figure S23. The average number of solvent molecules in substrate binding cleft of BSLA beneficial and non-beneficial substitutions during the MD simulations: (**a**) DMSO, and (**b**) Water. The number of DMSO/Water molecules was averaged over the last 40 ns from three independent MD runs.

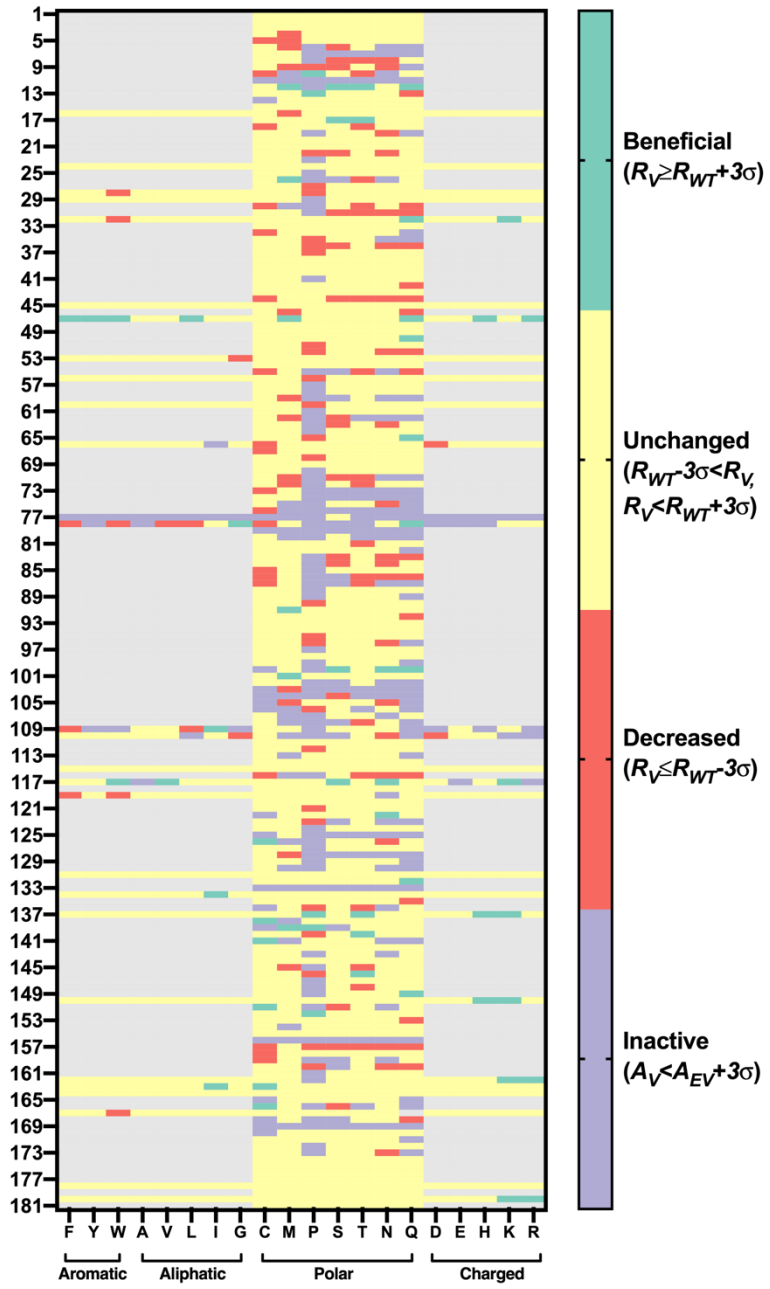

Figure S24. DOX resistance heatmap of BSLA surface polar-related substitutions. Residual activity, activity, variants, and the empty vector are denoted as R, A, V, and EV, respectively. The OS resistance was measured in the absence or presence of 22% (v/v) DOX cosolvents after 2 h incubation with crude culture supernatant. Amino acid is classified as follows: Aromatic: F, Y, W; Aliphatic: A, V, L, I, G; Polar: C, M, P, S, T, N, Q; Charged: D, E, K, H, R.

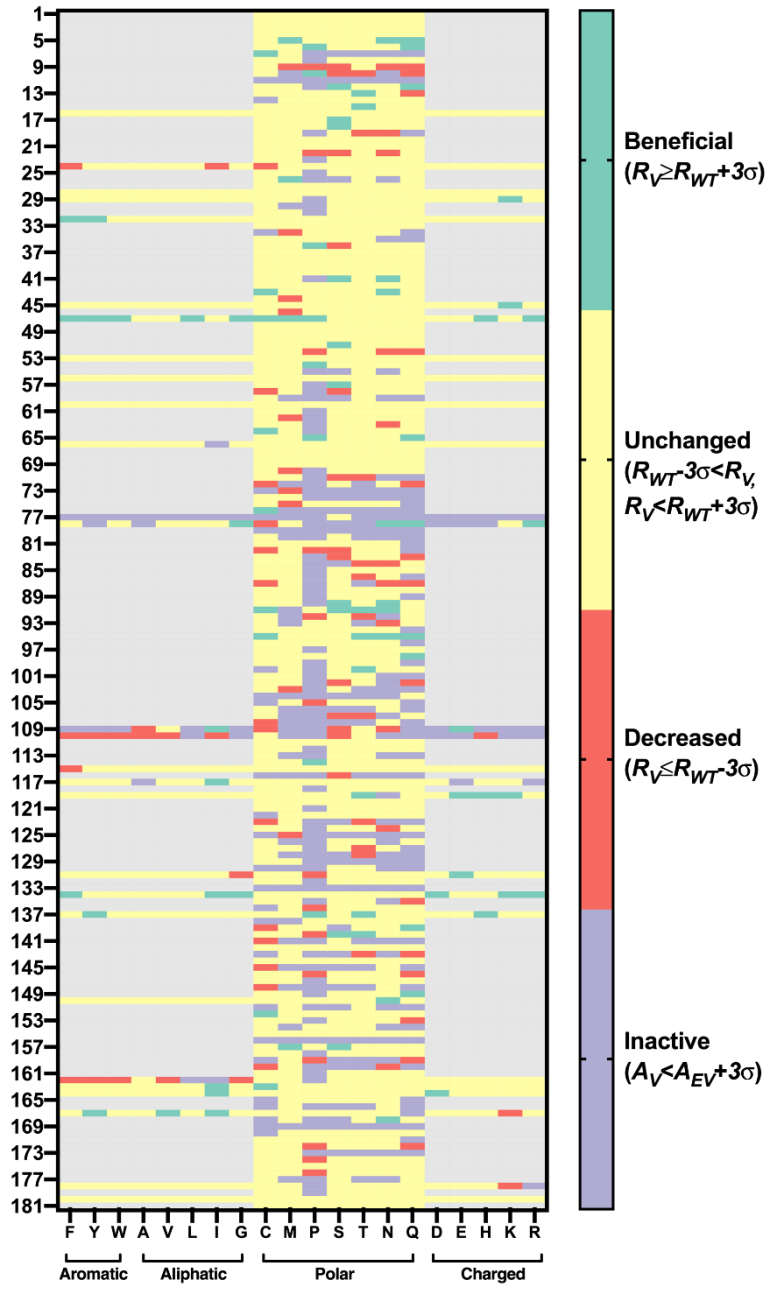

Figure S25. TFE resistance heatmap of BSLA surface polar-related substitutions. Residual activity, activity, variants, and the empty vector are denoted as R, A, V, and EV, respectively. The OS resistance was measured in the absence or presence of 12% (v/v) TFE cosolvents after 2 h incubation with crude culture supernatant. Amino acid is classified as follows: Aromatic: F, Y, W; Aliphatic: A, V, L, I, G; Polar: C, M, P, S, T, N, Q; Charged: D, E, K, H, R.

Reference

[1] H. Cui, T. H. J. Stadtmüller, Q. Jiang, K. E. Jaeger, U. Schwaneberg, M. D. Davari, *ChemCatChem* **2020**, *12*, 4073.

[2] H. Cui, L. Zhang, L. Eltoukhy, Q. Jiang, S. K. Korkunç, K.-E. Jaeger, U. Schwaneberg, M. D. Davari, *ACS Catal.* **2020**, *10*, 14847-14856.

[3] G. van Pouderoyen, T. Eggert, K. E. Jaeger, B. W. Dijkstra, *J. Mol. Biol.* **2001**, *309*, 215-226.

[4] V. J. Frauenkron-Machedjou, A. Fulton, J. Zhao, L. Weber, K.-E. Jaeger, U. Schwaneberg, L. Zhu, *Bioresour. Bioprocess.* **2018**, *5*, 2.

[5] W. Kabsch, C. Sander, *Biopolymers* **1983**, *22*, 2577-2637.

[6] J. Zhao, N. Jia, K. E. Jaeger, M. Bocola, U. Schwaneberg, *Biotechnol. Bioeng.* **2015**, *112*, 1997-2004.

[7] R. Guerois, J. E. Nielsen, L. Serrano, *J. Mol. Biol.* **2002**, *320*, 369-387.

[8] J. Van Durme, J. Delgado, F. Stricher, L. Serrano, J. Schymkowitz, F. Rousseau, *Bioinformatics* **2011**, *27*, 1711-1712.

[9] E. Krieger, G. Koraimann, G. Vriend, *Proteins: Struct., Funct., Bioinf.* **2002**, *47*, 393-402.

[10] H. Cui, H. Cao, H. Cai, K. E. Jaeger, M. D. Davari, U. Schwaneberg, *Chem. Eur. J* **2020**, *26*, 643-649.

[11] F. Eisenhaber, P. Lijnzaad, P. Argos, C. Sander, M. Scharf, *J. Comput. Chem.* **1995**, *16*, 273-284.